peroxiredoxin 1 that counteracts toxicity of mutant hungtington. *J Biol Chem* 287: 22717–22729, 2012.
36. Quaegebeur A, Segura I, and Carmeliet P. Pericytes: blood-brain barrier safeguards against neurodegeneration? *Neuron* 68: 321–323, 2010.
37. Quaegebeur A, Lange C, and Carmeliet P. The neurovascular link in health and disease: molecular mechanisms and therapeutic implications. *Neuron* 71: 406–424, 2011.
38. Rabilloud T, Heller M, Gasnier F, Luche S, Rey C, Aebersold R, Benahmed M, Louisot P, and Lunardi J. Proteomics analysis of cellular response to oxidative stress. Evidence for *in vivo* overoxidation of peroxiredoxins at their active site. *J Biol Chem* 277: 19396–19401, 2002.
39. Rani V, Neumann CA, Shao C, and Tischfield JA. Prdx1 deficiency in mice promotes tissue specific loss of heterozygosity mediated by deficiency in DNA repair and increased oxidative stress. *Mutat Res* 735: 39–45, 2012.
40. Riddell JR, Maier P, Sass SN, Moser MT, Foster BA, and Gollnick SO. Peroxiredoxin 1 stimulates endothelial cell expression of VEGF *via* TLR4 dependent activation of HIF-1α. *PLoS One* 7: e50394, 2012.
41. Rizzo MT and Leaver HA. Brain endothelial cell death: modes, signaling pathways, and relevance to neural development, homeostasis, and disease. *Mol Neurobiol* 42: 52–63, 2010.
42. Rott R, Szargel R, Haskin J, Bandopadhyay R, Lees AJ, Shani V, and Engelender S. α-Synuclein fate is determined by USP9X-regulated monoubiquitination. *Proc Natl Acad Sci U S A* 108: 18666–186671, 2011.
43. Satoh M, Fujimoto S, Haruna Y, Arakawa S, Horike H, Komai N, Sasaki T, Tsujioka K, Makino H, and Kashihara N. NAD (P) h oxidase and uncoupled nitric oxide syntase are major sources of glomerular superoxide in rats with experimental diabetic nephropathy. *Am J Physiol Renal Physiol* 288: F1144–F1152, 2005.
44. Schreibelt G, van Horssen J, Haseloff RF, Reijerkerk A, van der Pol SM, Nieuwenhuizen O, Krause E, Blasig IE, Dijkstra CD, Ronken E, and de Vries HE. Protective effects of peroxiredoxin-1 at the injured blood-brain barrier. *Free Radic Biol Med* 45: 256–264, 2008.
45. Shioda N, Han F, Moriguchi S, and Fukunaga K. Constitutively active calcineurin mediates delayed neuronal death through Fas-ligand expression *via* activation of NFAT and FKHR transcriptional activities in mouse brain ischemia. *J Neurochem* 102: 1506–1517, 2007.
46. Shirakura M, Murakami K, Ichimura T, Suzuki R, Shimoji T, Fukuda K, Abe K, Sato S, Fukasawa M, Yamakawa Y, Nishijima M, Moriishi K, Matsuura Y, Wakita T, Suzuki T, Howley PM, Miyamura T, and Shoji I. E6AP ubiquitin ligase mediates ubiquitylation and degradation of hepatitis C virus core protein. *J Virol* 81: 1174–1185, 2007.
47. Sultana R, Perluigi M, Newman SF, Pierce WM, Cini C, Coccia R, and Butterfield DA. Redox proteomic analysis of carbonylated brain proteins in mild cognitive impairment and early Alzheimer's disease. *Antioxid Redox Signal* 12: 327–336, 2010.
48. Tan KH, Harrington S, Purcell WM, and Hurst RD. Peroxinitrite mediates nitric oxide-induced blood-brain barrier damage. *Neurochem Res* 29: 579–587, 2004.
49. Tao RR, Ji YL, Lu YM, Fukunaga K, and Han F. Targeting nitrosative stress for neurovascular protection: new implications in brain diseases. *Curr Drug Targets* 13: 272–284, 2012.
50. Wilcox CS and Pearlman A. Chemistry and antihypertensive effects of tempol and other nitroxides. *Pharmacol Rev* 60: 418–469, 2008.
51. Zhang GS, Tian Y, Huang JY, Tao RR, Liao MH, Lu YM, Ye WF, Wang R, Fukunaga K, Lou YJ, and Han F. The γ-Secretase blocker DAPT reduces the permeability of the blood-brain barrier by decreasing the ubiquitination and degradation of occludin during permanent brain ischemia. *CNS Neurosci Ther* 19: 53–60, 2012.

Address correspondence to:
Dr. Feng Han
Institute of Pharmacology, Toxicology and Biochemical Pharmaceutics
Zhejiang University
Hangzhou 310058
China

E-mail: changhuahan@zju.edu.cn

Date of first submission to ARS Central, April 18, 2013; date of final revised submission, November 12, 2013; date of acceptance, December 2, 2013.

Abbreviations Used

ASK1 = apoptosis signal-regulating kinase 1
BBB = blood–brain barrier
DAPI = 4′,6-diamidino-2-phenylindole
DMEM = Dulbecco's modified Eagle's medium
E6AP = E6-associated protein
ER = endoplasmic reticulum
FKHR = forkhead transcription factor Foxo1
H_2O_2 = hydrogen peroxide
HBMEC = human brain microvascular endothelial cell
HO-1 = heme oxygenase-1
HSP27 = heat shock protein 27
JNK = c-Jun N-terminal kinase
MALDI-TOF = matrix-assisted laser desorption/ionization-time-of-flight
mHtt = mutant Hungtington
MMPs = metalloproteinases
NeuN = neuronal nuclear marker
NO = nitric oxide
Nrf2 = NF-E2-related factor 2
$O_2^{\bullet-}$ = superoxide
OGD = oxygen–glucose deprivation
$ONOO^-$ = peroxynitrite
PAGE = polyacrylamide gel electrophoresis
PARP = poly ADP-ribose polymerase
PBS = phosphate-buffered saline
PI = propidium iodide
Prx = peroxiredoxin
ROS = reactive oxygen species
SDS = sodium dodecyl sulfate
shRNA = short hairpin RNA
SIN-1 = 3-morpholinosydnonimine
siRNA = small interfering RNA
tMCAO = transient middle cerebral artery occlusion
TUNEL = terminal deoxynucleotidyl transferase dUTP nick end labeling
ZO-1 = zonula occludens-1

Published September 15, 2014

JEM

Article

Selective and strain-specific NFAT4 activation by the *Toxoplasma gondii* polymorphic dense granule protein GRA6

Ji Su Ma,[1,2,3,4] Miwa Sasai,[1,2] Jun Ohshima,[1,2,5] Youngae Lee,[2] Hironori Bando,[1] Kiyoshi Takeda,[3,4,6] and Masahiro Yamamoto[1,2]

[1]Department of Immunoparasitology, Research Institute for Microbial Diseases, [2]Laboratory of Immunoparasitology, [3]Laboratory of Mucosal Immunology, WPI Immunology Frontier Research Center, [4]Department of Microbiology and Immunology, Graduate School of Medicine, and [5]Department of Restorative Dentistry and Endodontology, Osaka University Graduate School of Dentistry, Suita, Osaka 565-0871, Japan
[6]Core Research for Evolutional Science and Technology, Japan Science and Technology Agency, Saitama 332-0012, Japan

***Toxoplasma gondii* infection results in co-option and subversion of host cellular signaling pathways. This process involves discharge of *T. gondii* effector molecules from parasite secretory organelles such as rhoptries and dense granules. We report that the *T. gondii* polymorphic dense granule protein GRA6 regulates activation of the host transcription factor nuclear factor of activated T cells 4 (NFAT4). GRA6 overexpression robustly and selectively activated NFAT4 via calcium modulating ligand (CAMLG). Infection with wild-type (WT) but not *GRA6*-deficient parasites induced NFAT4 activation. Moreover, *GRA6*-deficient parasites failed to exhibit full virulence in local infection, and the treatment of WT mice with an NFAT inhibitor mitigated virulence of WT parasites. Notably, *NFAT4*-deficient mice displayed prolonged survival, decreased recruitment of CD11b$^+$ Ly6G$^+$ cells to the site of infection, and impaired expression of chemokines such as Cxcl2 and Ccl2. In addition, infection with type I parasites culminated in significantly higher NFAT4 activation than type II parasites due to a polymorphism in the C terminus of GRA6. Collectively, our data suggest that GRA6-dependent NFAT4 activation is required for *T. gondii* manipulation of host immune responses to maximize the parasite virulence in a strain-dependent manner.**

CORRESPONDENCE
Masahiro Yamamoto:
myamamoto@
biken.osaka-u.ac.jp

Abbreviations used: CAMLG, calcium modulating ligand; CsA, cyclosporin A; dpLN, draining popliteal LN; gRNA, guide RNA; MNN, membranous nanotubular network; PV, parasitophorous vacuole; PVM, PV membrane.

Toxoplasma gondii (*T. gondii*) is the causative agent of toxoplasmosis, a condition including life-threatening encephalitis, pneumonia, and myocarditis in immunocompromised individuals, such as those suffering from acquired immunodeficiency syndrome and being treated by chemotherapy (Boothroyd, 2009). Furthermore, primary infection with this pathogen during pregnancy in humans and animals also leads to congenital diseases such as hydrocephalus and chorioretinitis in newborn children (Montoya and Remington, 2008). *T. gondii* is an obligatory intracellular protozoan parasite and taxonomically belongs to the phylum Apicomplexa, which is defined by the presence of an apical complex including secretory organelles (Boothroyd and Dubremetz, 2008). Among them, the large bulb-shaped organelles, rhoptries, possess several proteins called ROPs, in which more than 40 members, such as ROP5, ROP16, ROP18, and ROP38, harbor protein kinase domains (Peixoto et al., 2010). ROPs are secreted into the host cytoplasm during parasite invasion and eventually localize at the host nucleus or parasite-forming nonfusogenic vacuoles called parasitophorous vacuoles (PVs) to subvert and co-opt host cell functions (Dubremetz, 2007; Hunter and Sibley, 2012; Kemp et al., 2013).

Dense granules are another type of parasite secretory organelles that discharge GRA proteins (GRAs) into PVs that contain a network of elongated nanotubular structures (Cesbron-Delauw et al., 2008). The membranes of nanotubules are connected by PV membranes (PVMs), resulting in the formation of a large interface between host cell cytoplasm and parasite (Sibley et al., 1995; Mercier et al., 2002). Some GRAs,

J.S. Ma and M. Sasai contributed equally to this paper.

The Rockefeller University Press $30.00
J. Exp. Med. 2014 Vol. 211 No. 10 2013-2032
www.jem.org/cgi/doi/10.1084/jem.20131272

Supplemental Material can be found at:
http://jem.rupress.org/content/suppl/2014/09/12/jem.20131272.DC1.html

Published September 15, 2014

JEM

A

	Full-length (Amino acid)	Signal peptide Predicted by ToxoDB	Region cloned in expression vector	Strain used to isolate cDNA
GRA1	190	1-25	30-190	RH
GRA2	185	1-24	40-185	RH
GRA3	222	1-43	44-222	RH
GRA4	332	1-21	25-332	RH
GRA5	120	1-27	20-120	RH
GRA6	230	No	1-230 (Full)	RH
GRA7	236	1-27	28-236	RH
GRA8	267	1-24	28-267	RH
GRA9	318	1-19	20-318	RH
GRA10	894	No	1-894 (Full)	RH
GRA12	436	1-39	22-436	RH
GRA14	408	1-36	30-408	RH
GRA15	550	No	51-550	ME49

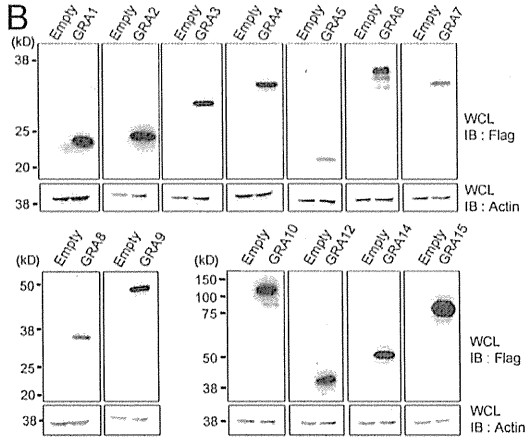

C

	NF-κB	ISRE	SRF	C/EBP	SRE	NFAT	TPU	CRE	GAS	UPRE	TARE	IFN-β	DR1	DR3	DR4	DR5	LILRE	Egr1	GRE
GRA1	0.5	1	1	2	1	1	2	0.4	1	1	2	1	1	1	1	1	1	1	1
GRA2	1	1	1	1	1	1	1	1	1	1	1	1	1	1	1	1	1	1	1
GRA3	3	1	2	1	3	8	2	2	3	1	1	2	3	3	4	3	1	3	3
GRA4	1	1	1	1	1	2	1	1	1	3	2	1	1	1	1	2	1	1	1
GRA5	1	1	2	2	5	1	2	1	1	1	2	1	2	2	2	1	2	1	2
GRA6	81	2	5	4	86	2844	12	48	18	5	4	5	11	14	14	11	1	12	14
GRA7	3	2	1	1	1	5	1	1	1	1	1	1	1	1	2	1	1	1	1
GRA8	2	1	1	1	1	2	1	1	1	2	1	1	1	1	1	1	1	1	1
GRA9	0.4	1	1	1	1	2	1	1	0.5	1	1	1	1	1	1	1	1	1	1
GRA10	1	1	1	2	1	1	1	1	1	1	3	2	2	2	1	3	1	1	1
GRA12	5	1	1	1	1	21	2	3	1	3	2	3	3	4	3	3	1	2	3
GRA14	246	1	1	1	2	235	2	4	3	1	1	9	3	9	4	4	1	3	4
GRA15	3148	3	1	6	5	9	6	11	3	19	4	18	5	9	5	5	2	5	12

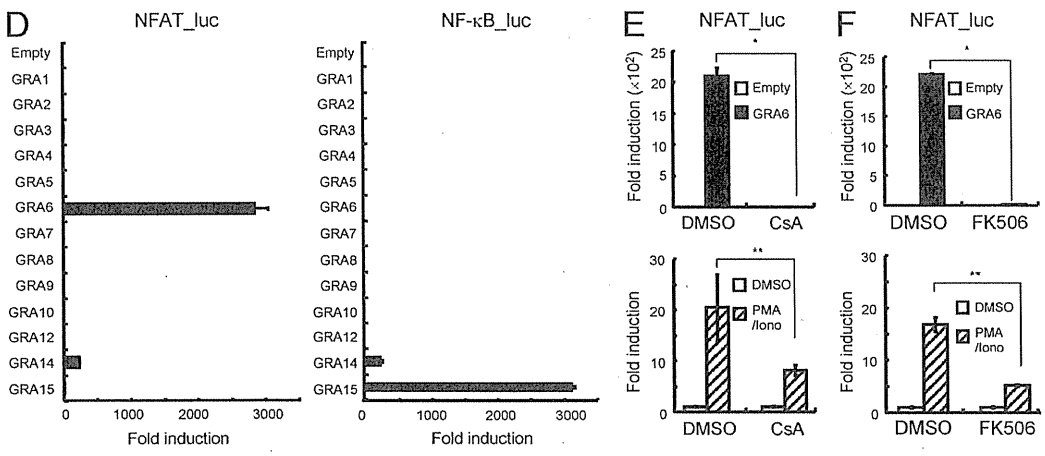

Figure 1. Overexpression of GRA6 strongly activates the NFAT-dependent promoter. (A) A list of GRAs tested in this study. Regions excluding signal peptides predicted by ToxoDB were shown in the center column, amplified using cDNA derived from RH or ME49 *T. gondii*, and cloned in mammalian expression plasmids. (B) Lysates of 293T cells transiently transfected with Flag-tagged GRA expression plasmids were subjected to Western blot using indicated Abs. (C) 293T cells were transfected with indicated luciferase reporters together with indicated expression vectors for GRAs. Luciferase activities were expressed as fold increases over the background levels shown by lysates prepared from mock-transfected cells. (D) 293T cells were transfected with luciferase reporters for NFAT (left) or NF-κB (right) together with indicated GRA expression vectors. Luciferase activities were expressed as indicated above. Error bars represent means ± SD of triplicates. (E and F) 293T cells were transfected with the NFAT-luc reporter together with empty or GRA6 expression vectors (top) treated with PMA/ionophore (bottom) in the presence of 100 ng/ml CsA (E) or 0.5 ng/ml FK506 (F) or DMSO (control). Luciferase activities were expressed as indicated above. Error bars represent means ± SD of triplicates. *, $P < 0.005$; **, $P < 0.05$, determined by unpaired Student's *t* test in E or F. Data are representative of three (D) and two (B, C, E, and F) independent experiments.

Published September 15, 2014

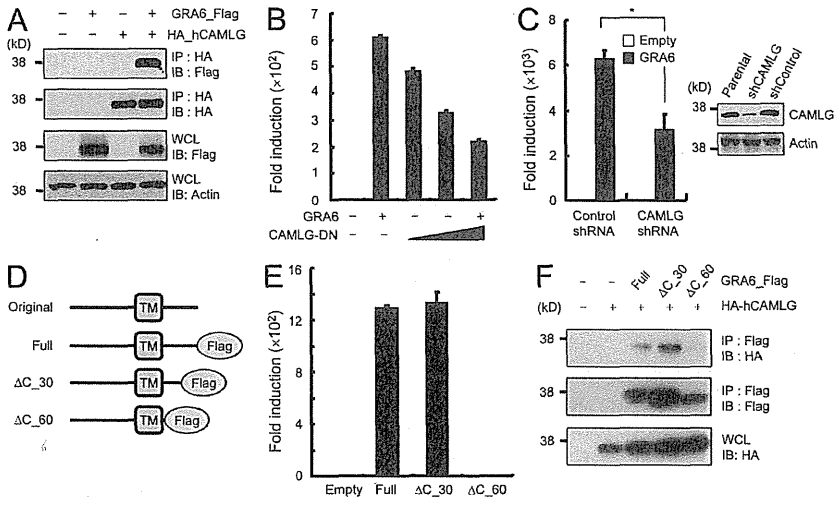

Figure 2. CAMLG is required for the GRA6-mediated NFAT activation. (A) Lysates of 293T cells transiently cotransfected with Flag-tagged GRA6 and/or HA-tagged CAMLG were immunoprecipitated with the indicated Abs and subjected to Western blot. (B) 293T cells were transfected with the NFAT-dependent luciferase reporter together with indicated expression vectors. Luciferase activities were expressed as indicated above. Error bars represent means ± SD of triplicates. (C) 293T cells stably expressing shRNA for human CAMLG or control were transfected with the NFAT-dependent luciferase reporter together with empty or GRA6 expression vectors. Luciferase activities were expressed as indicated above. Error bars represent means ± SD of triplicates. Lysates of 293T cells stably expressing shRNA for human CAMLG or control were subjected to Western blot. (D) Flag-tagged GRA6 variants. TM, transmembrane. (E) 293T cells were transfected with the NFAT-dependent luciferase reporter together with indicated expression vectors. Luciferase activities were expressed as indicated above. Error bars represent means ± SD of triplicates. (F) Lysates of 293T cells transiently cotransfected with Flag-tagged indicated GRA6 vectors and/or HA-tagged CAMLG were immunoprecipitated with the indicated Abs. *, $P < 0.005$ determined by unpaired Student's *t* test in C. Data are representative of three (A–C) and two (E and F) independent experiments.

such as GRA3, 5, 7, 8, 10, and 14, have been shown to be located at the PVMs. Conversely, GRA2, 4, 6, 9, and 12 are localized to the membrane of the nanotubule network (Labruyere et al., 1999; Mercier et al., 2005). Among them, GRA2 and GRA6 play a central role in the formation and stabilization of the nanotubule network, respectively (Mercier et al., 2002). In addition to being associated with the membranous interface between PVs and the host cytoplasm, two new GRA family members, GRA15 and GRA16, were recently shown to participate in the modulation of host cell functions. GRA15 is involved in NF-κB activation, which promotes the production of proinflammatory cytokines (Rosowski et al., 2011). The mode of action by which GRA15 activates NF-κB remains uncertain; however, it is dependent on a strong NF-κB activating signal transducer, TRAF6, but independent of the essential adaptors for Toll-like receptors, MyD88 and TRIF (Rosowski et al., 2011). GRA16 is secreted from dense granules and eventually exported to the host nucleus, where GRA16 interacts with the host deubiquitinase HAUSP and PP2A phosphatase, which regulate host cell cycle progression and the p53 tumor suppressor signaling pathway (Bougdour et al., 2013). Very recently, GRA24 is shown to modulate host immune responses by promoting p38 MAP kinase activation (Braun et al., 2013). Thus, GRAs, as well as ROPs, modulate host cell signaling pathways (Melo et al., 2011; Hunter and Sibley, 2012).

T. gondii has been divided into three archetypal lineages (types I, II, and III) that predominate in North America and Europe (Howe and Sibley, 1995). However, strains of clinical and field isolates from human patients and animals in South America and Africa were revealed to comprise distinct lineages from the three major lines (Dardé, 2008). Furthermore, a recent study demonstrates that globally diverse *T. gondii* isolates consist of six major clades (Su et al., 2012). To genetically characterize these nonarchetypal strains, molecular biological methods using PCR-based genotyping or serological tests using strain-specific peptides at multiple polymorphic loci have been developed (Kong et al., 2003; Dardé, 2004). Regarding GRAs, polymorphisms in the sequences of *GRA3*, *GRA5*, *GRA6*, *GRA7*, and *GRA15* genes have been reported (Kong et al., 2003; Peyron et al., 2006; Sousa et al., 2009; Rosowski et al., 2011). Among them, GRA6 contains a high number of polymorphisms that are widely used in typing *T. gondii* isolates (Fazaeli et al., 2000; Miller et al., 2004; Lin et al., 2005; Khan et al., 2006; Petersen et al., 2006; Belfort-Neto et al., 2007; Dubey et al., 2007; Sousa et al., 2008). Here, we demonstrate that *T. gondii* GRA6 triggers the host signaling pathway for activation of a host transcription factor, nuclear factor of activated T cells 4 (NFAT4), which is required for the full virulence by the local infection of *T. gondii*, and that a polymorphism in the C terminus of GRA6 is associated with strain-specific NFAT4 activation.

RESULTS

Ectopic expression of GRA6 robustly activates the NFAT-dependent promoter in 293T cells

T. gondii GRA proteins, such as GRA15, GRA16, and GRA24, were recently shown to directly influence gene expression in host cells (Rosowski et al., 2011; Bougdour et al., 2013). We hypothesized that GRA proteins other than GRA15, GRA16, and GRA24 also manipulate host gene expression by activating signaling pathways in host cells. We previously showed that ectopic expression of ROP16, which is involved in Stat3-dependent suppression of host innate immunity (Yamamoto et al., 2009), also activates a Stat3-dependent promoter in mammalian cells, indicating that the heterologous

Published September 15, 2014

expression of *T. gondii* proteins in mammalian cells may correctly recapitulate the biological effects of infection on signal transduction. Therefore, we constructed mammalian expression vectors for GRA proteins other than GRA11, GRA13, GRA16, and GRA24, and checked their expression in 293T cells by Western blotting (Fig. 1, A and B). Then, we assessed whether their overexpression, together with luciferase reporter plasmids harboring elements dependent on various transcription factors, activates the reporters (Fig. 1 C). Consistent with a previous report showing that GRA15 is involved in activation of NF-κB (Rosowski et al., 2011), overexpression of GRA15 strongly up-regulated the activity of the NF-κB–dependent ELAM promoter (Fig. 1, C and D). Intriguingly, ectopic expression of GRA6 dramatically and preferentially activated the NFAT-dependent promoter (Fig. 1, C and D). NFATs are a family of transcription factors that play important roles in immunity and several developmental processes in vertebrates (Müller and Rao, 2010). Activation of NFATs, except for NFAT5, requires dephosphorylation by calcineurin, whose activity is inhibited by cyclosporine A (CsA) and FK506 (Clipstone and Crabtree, 1992; Jain et al., 1993). We tested whether GRA6-mediated activation of the NFAT-dependent promoter is inhibited by these compounds. Addition of CsA or FK506 resulted in suppression of the NFAT-dependent activation mediated by GRA6 as well as PMA/ionophore (Fig. 1, E and F). Collectively, these findings reveal that ectopic expression of GRA6 robustly induces activation of the NFAT-dependent promoter in a calcineurin-dependent manner.

Calcium modulating ligand (CAMLG) is involved in GRA6-mediated NFAT activation

We next analyzed the molecular mechanism by which GRA6 overexpression mediates activation of the NFAT-dependent promoter. A previous study using a yeast two-hybrid screen identified CAMLG as a GRA6-interacting protein (Ahn et al., 2006). CAMLG was originally reported to be engaged in the activation of NFAT (Bram and Crabtree, 1994). Indeed, our immunoprecipitation study revealed an interaction between Flag-tagged GRA6 and HA-tagged human CAMLG in 293T cells (Fig. 2 A). Moreover, coexpression of a dominant-negative form of CAMLG and suppression of CAMLG expression by shRNA inhibited GRA6-mediated activation of the NFAT-dependent promoter (Fig. 2, B and C), indicating that CAMLG is important for GRA6-induced NFAT activation. Next, we analyzed which portion of GRA6 is required for NFAT activation. GRA6 is predicted to contain a transmembrane domain and a cytoplasmic C-terminal domain (Gendrin et al., 2010). Deletion mutants of GRA6 lacking the C-terminal 30 or 60 amino acids (named ΔC_30 or ΔC_60, respectively) were generated and tested for NFAT activity (Fig. 2 D). The full-length and ΔC_30 proteins, but not ΔC_60, activated the NFAT-dependent promoter (Fig. 2 E). Regarding the interaction with CAMLG, the full-length and ΔC_30 Flag-tagged proteins, but not Flag-tagged ΔC_60, associated with HA-tagged CAMLG (Fig. 2 F). Thus, CAMLG is involved in NFAT activation by interacting with the C-terminal portion of GRA6.

The GRA6–CAMLG axis preferentially activates NFAT4 in mammalian cells

NFAT consists of five family members (NFAT1, NFAT2, NFAT3, NFAT4, and NFAT5), among which NFAT1–4 are tightly regulated by calcineurin (Lopez-Rodríguez et al., 1999). We assessed whether the GRA6–CAMLG axis universally or selectively activates NFAT members. Expression of individual NFAT expression vectors alone in 293T cells only resulted in strong activation of the NFAT-dependent reporter after NFAT3 overexpression. However, the coexpression of CAMLG with NFAT4, but not with other members of the NFAT family, led to synergistic activation of the promoter to a similar extent to that achieved by GRA6 (Fig. 3 A), whereas introduction of individual NFAT expression vectors in concert with PMA/ionophore stimulation robustly activated the NFAT-dependent promoter (Fig. 3 B). In addition, HA-tagged CAMLG coprecipitated with endogenous NFAT4, but not other NFAT members (Fig. 3, C and D), probably conferring the specific NFAT4 activation on the CAMLG overexpression. We next examined whether GRA6-dependent NFAT activation is affected by knockdown of individual NFAT members (Fig. 3 E). We found that GRA6-mediated activation of the NFAT-dependent promoter was selectively suppressed by down-regulation of *NFAT4* gene expression but not by down-regulation of other NFAT members (Fig. 3 F). Moreover, ectopic expression of GRA6 in MEFs expressing RFP-tagged NFAT4 culminated in nuclear translocation (Fig. 3 G). Collectively, these results implicated GRA6 in the CAMLG-dependent selective activation of NFAT4 in mammalian cells.

GRA6 is essential for NFAT4 activation after *T. gondii* infection in MEFs

The fact that heterologous GRA6 overexpression mediates NFAT4 activation in mammalian cells prompted us to examine whether this transcription factor is activated by *T. gondii* infection. In response to infection with the type I RH strain of *T. gondii*, nuclear translocation of NFAT4 was observed in MEFs (Fig. 4 A). To evaluate whether type I *T. gondii* infection-induced NFAT4 activation is dependent on GRA6, we generated *GRA6*-deficient parasites by gene targeting (Fig. 4, B–D). *GRA6*-deficient parasites exhibited formation of plaques on MEFs, time-dependent growth, and similar numbers of parasites per PV to WT parasites (Fig. 4, E–G). We then assessed NFAT4 activation in MEFs infected with WT or *GRA6*-deficient parasites (Fig. 4, J and K). We found that the nuclear translocation of NFAT4 was significantly reduced in cells infected with *GRA6*-deficient parasites in comparison with those infected with WT parasites (Fig. 4, J and K). To confirm that the defective NFAT4 activation in *GRA6*-deficient parasites is a consequence of *GRA6* deficiency, we reintroduced a *GRA6* gene into the endogenous locus in *GRA6*-deficient parasites (Fig. 4, H and I). Reintroduction of GRA6 into *GRA6*-deficient parasites resulted in the restoration of NFAT4 nuclear translocation after infection (Fig. 4, J and K), indicating the important role of GRA6 in the NFAT4 activation induced by *T. gondii*–infected cells.

Published September 15, 2014

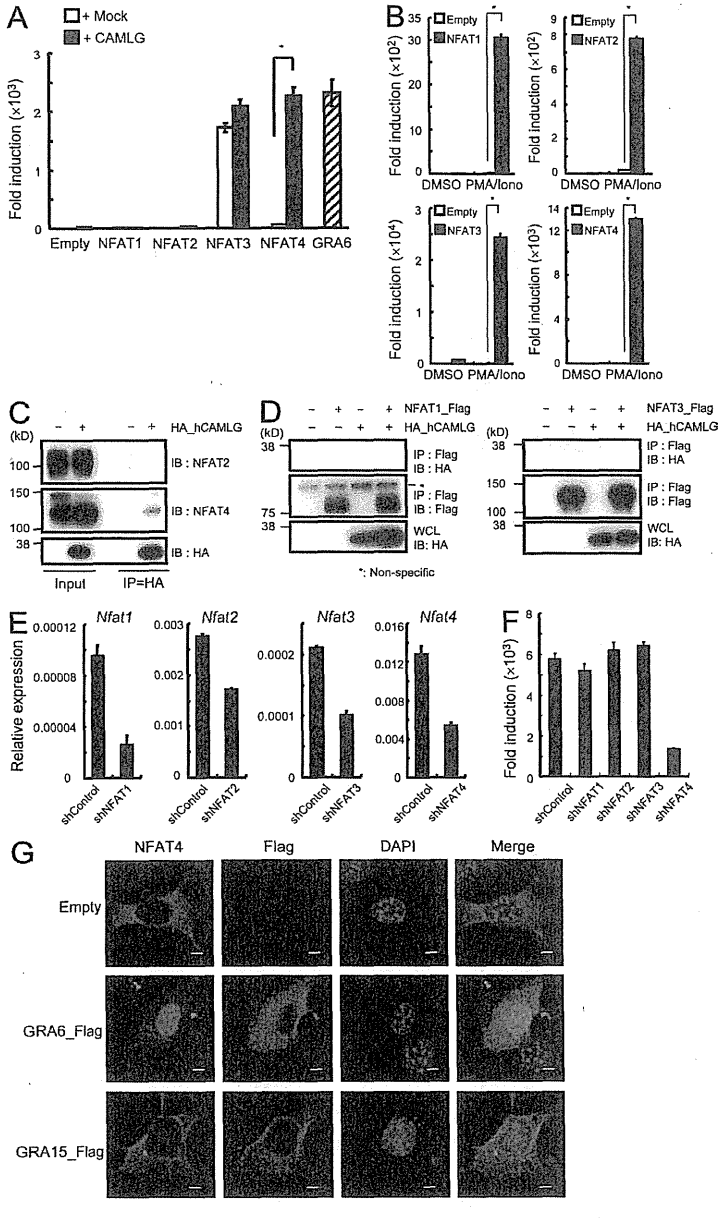

Figure 3. NFAT4 is selectively activated by ectopic expression of GRA6. (A) 293T cells were transfected with the NFAT-dependent luciferase reporter together with indicated expression vectors. Luciferase activities in the presence or absence of CAMLG were expressed as indicated above. Error bars represent means ± SD of triplicates. (B) 293T cells were transfected with the NFAT-dependent luciferase reporter together with indicated expression vectors. Luciferase activities in the presence or absence of PMA/ionophore were expressed as indicated above. Error bars represent means ± SD of triplicates. (C) Lysates of 293T cells transiently transfected with HA-tagged CAMLG were immunoprecipitated with the indicated Abs and subjected to Western blotting. (D) Lysates of 293T cells transiently cotransfected with Flag-tagged indicated NFAT vectors and/or HA-tagged CAMLG were immunoprecipitated with the indicated Abs and subjected to Western blot. (E) Quantitative RT-PCR analysis was performed using cDNA reversely transcribed from RNA extracted from 293T cells stably expressing shRNA for control or NFAT1-4. Relative mRNA levels of indicated genes compared with the *GAPDH* level were shown in the y axis. Error bars represent means ± SD of triplicates. (F) 293T cells stably expressing shRNA for human NFAT1-4 or control were transfected with the NFAT-dependent luciferase reporter together with empty or GRA6 expression vectors. Error bars represent means ± SD of triplicates. (G) MEFs stably expressing RFP-tagged NFAT4 were transfected with empty or Flag-tagged GRA6 or GRA15 expression vectors. 24 h after transfection, the cells were fixed and stained with mouse anti-Flag, and then Alexa Fluor 488–conjugated anti-mouse IgG (green) or DAPI (blue). Bars, 5 µm. *, $P < 0.001$, determined by unpaired Student's *t* test in A or B. Data are representative of three (A and F) and two (B–E and G) independent experiments.

GRA6 mediates full virulence in mice locally infected with type I *T. gondii*

To assess the role of GRA6 in in vivo virulence in mice, BALB/c mice were infected with WT or *GRA6*-deficient type I parasites expressing a firefly luciferase. We then monitored the in vivo spreading of the parasite and the survival rate. Intraperitoneal infection resulted in comparable spreading and survival rates between the two groups (Fig. 5, A–C). In sharp contrast, we found that local infection, in which parasites were injected into the right footpad, culminated in significantly slower systemic diffusion of *GRA6*-deficient parasites than that of WT parasites (Fig. 5 ,D and E). In addition, mice locally infected with *GRA6*-deficient parasites survived for significantly longer than did those infected with WT parasites (Fig. 5 F). The delayed mortality caused by GRA6 deficiency was resolved by the restoration of GRA6 in *GRA6*-deficient parasites (Fig. 5 F). Furthermore, BALB/c mice subcutaneously inoculated with *GRA6*-deficient parasites displayed significantly delayed parasite spreading and mortality, compared with the WT parasite-infected mice (Fig. 5, G–I).

We next examined whether the decrease in virulence caused by GRA6 deficiency is related to NFAT activity. CsA treatment of 293T cells strongly inhibited activation of the NFAT-dependent promoter by GRA6 overexpression (Fig. 1 E)

Published September 15, 2014

JEM

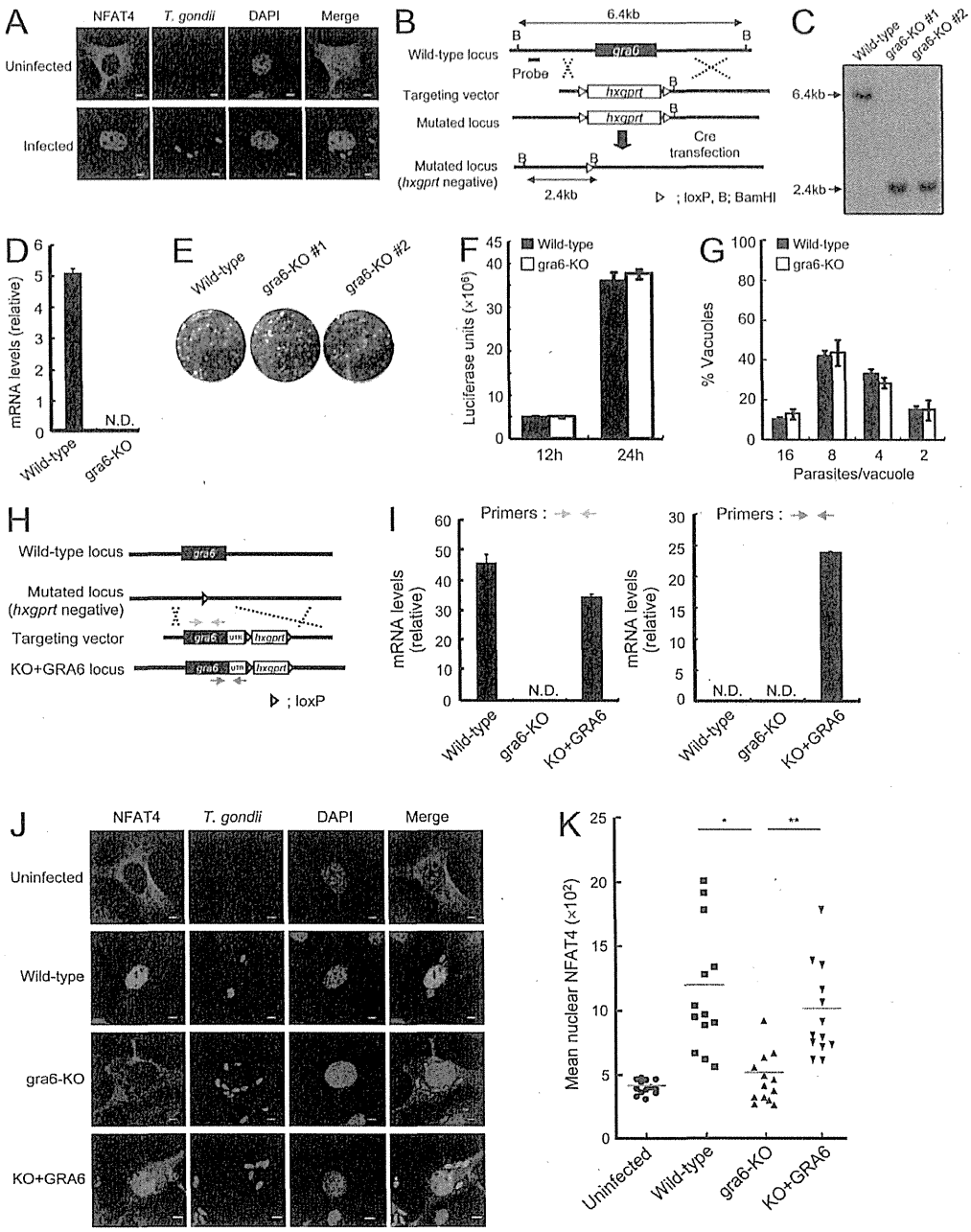

Figure 4. NFAT4 activation by *T. gondii* infection is dependent on GRA6. (A) MEFs stably expressing RFP-NFAT4 were uninfected or infected with *T. gondii* (moi = 5), fixed at 6 h after infection, and stained with DAPI. Bars, 5 µm. (B) Structure of the *GRA6* gene, targeting vector, and predicted disrupted gene. Black boxes denote the exon. Restriction enzymes: B, BamHI. (C) Southern blot analysis of offspring from WT or two lines of *GRA6*-deficient parasites. Total genomic DNA was extracted from parasites, digested with BamHI, electrophoresed, and hybridized with the radiolabeled probe indicated in B. Southern blotting gave a single 2.4-kb band for WT and a 6.4-kb band for the disrupted locus. (D) Quantitative RT-PCR analysis was performed using cDNA reversely transcribed from RNA extracted from WT and gra6-ko parasites. Relative mRNA levels of *GRA6* compared with the *α-tubulin* level were shown in the y axis. Error bars represent means ± SD of triplicates. N.D., not detected. (E) Plaque assays. MEF monolayers were infected with WT or two independent gra6-KO parasites (#1 and #2), and then fixed after 8 d and stained with crystal violet. (F) Total number of WT or gra6-KO parasites infecting in MEFs were measured by luciferase assay after indicated hours after infection. Error bars represent means ± SD of triplicates. (G) Intracellular growth assays. Replication was analyzed 24 h after infection. Error bars represent means ± SD of triplicates. (H) Targeting vector complementing GRA6 and harboring the endogenous promoter. Black boxes denote the exon. Blue and red primers were used to measure mRNAs for *GRA6* and a region specifically

Published September 15, 2014

and the nuclear translocation of NFAT4 after infection of MEFs with WT *T. gondii* (Fig. 6, A and B). Then, we systemically treated BALB/c mice with CsA and challenged them with WT parasites. We found that, compared with the control group, CsA-treated mice exhibited delayed spreading of WT parasites and prolonged survival, reminiscent of infection with *GRA6*-deficient parasites (Fig. 6, C–E). In sharp contrast, CsA treatment did not affect parasite spread or survival rates in mice infected intraperitoneally (Fig. 6, F–H). Moreover, the CsA treatment had no effect on parasite dissemination or mortality in mice locally infected with *GRA6*-deficient parasites (Fig. 6, I–K). Collectively, these results suggest that GRA6 plays an important role in local infection-induced full virulence, and the local infection-induced virulence inhibited by the CsA treatment is dependent on the presence of GRA6.

GRA6-dependent recruitment of CD11b$^+$ Ly6G$^+$ cells to the infection site

In our local footpad infection model, WT parasites spread from the site of infection (footpad) gradually to the whole body (Fig. 5 D). When the luciferase signal emitted from WT parasites began to be detected in the legs of the infected side, the size of the draining popliteal LNs (dpLNs) from mice infected with WT parasites was larger than that of mice infected with *GRA6*-deficient parasites or of CsA-treated mice infected with WT parasites (Fig. 7 A). Next, we tested those dpLNs for the parasite presence by flow cytometry. Consistent with the in vivo imaging analysis, dpLNs from mice infected with WT parasites contained higher frequency of live cells infected with parasites than those from *GRA6*-deficient parasite-infected mice or from CsA-treated mice infected with WT parasites (Fig. 7 B), suggesting that the GRA6–NFAT4 axis might be involved in the parasite spread from the footpad to the dpLNs. Because *T. gondii* is considered to use the migratory ability of CD11b$^+$ cells to spread from the infected site to systemic (Courret et al., 2006; Bierly et al., 2008; Coombes et al., 2013), we examined whether the *T. gondii*–infected live cell population contains CD11b$^+$ cells. Then we found that nearly half of the *T. gondii*–infected live cell population was positive for CD11b (Fig. 7 B). It has been reported that CD11b$^+$ cells are recruited to the site of infection before the parasite spread (Courret et al., 2006), prompting us to analyze whether CD11b$^+$ cells are accumulated in the footpads in local infection at an early time point when little if any parasite signal was measured by in vivo imaging analysis. We detected considerable proportion and numbers of CD11b$^+$ Ly6G$^+$ cells in footpads of mice infected with WT parasites (Fig. 7, C–E). In contrast, the CD11b$^+$ Ly6G$^+$ cell numbers in *GRA6*-deficient parasite-infected footpads were markedly decreased (Fig. 7, C–E), indicating that the GRA6–NFAT4 axis may control the accumulation of CD11b$^+$ Ly6G$^+$ cells in the infected footpad.

GRA6-dependent induction of Cxcl2 and Ccl2 chemokines

Recruitment of CD11b$^+$ cells, including neutrophils and monocytes, is regulated by small cytokines such as CXC and CC chemokines (Zlotnik and Yoshie, 2000). Therefore, we examined the induction of these chemokines in the footpads infected with WT or *GRA6*-deficient parasites (Fig. 7 F). The mRNA expression levels of *Cxcl2* and *Ccl2* in the footpads of mice infected with WT parasites were markedly higher than those in the footpads infected with *GRA6*-deficient parasites (Fig. 7 F). Furthermore, the CsA treatment in WT parasite-infected mice resulted in significant reduction in induction of these chemokines in the footpad (Fig. 7 F). Next, we addressed whether the defective Cxcl2 and Ccl2 induction by the *GRA6* deficiency is cell-intrinsic. To test this, we tested expression levels of chemokines, including Cxcl2 and Ccl2, in *T. gondii*–infected fibroblasts because CD11b-negative cells were infected in the footpad at early time points after infection (Fig. 7, G and H; and not depicted). Infection of WT parasites in fibroblasts induced mRNAs of various chemokines (Fig. 7 G). Among them, we found that induction of Cxcl2 and Ccl2 was specifically retarded in cells infected with *GRA6*-deficient parasites (Fig. 7 G). Moreover, the CsA treatment in cells led to a significant defect in the expression of these chemokines in response to WT parasite infection (Fig. 7 H), suggesting that the GRA6-dependent NFAT4 activation may be involved in induction of Cxcl2 and Ccl2.

NFAT4 is essential for the full virulence by the local infection of WT parasites

To test whether NFAT4 is required for the GRA6-dependent full virulence directly, we generated NFAT4-deficient mice by the Cas9/CRISPR-mediated genome editing (Cong et al., 2013). A guide RNA (gRNA) was designed within the second exon of murine *Nfat4* gene and injected into one-cell embryos of mice together with mRNA of the RNA-guided endonuclease Cas9 (Wang et al., 2013). We screened the resultant pops and isolated a pup possessing 4 bp insertion in the targeted region of *Nfat4* gene (Fig. 8 A). The pop with the mutated *Nfat4* allele was crossed with C57BL/6 mice to obtain a group of heterozygous mice, which were intercrossed

derived from the targeting vector, respectively. (I) Quantitative RT-PCR analysis was performed using cDNA reversely transcribed from RNA extracted from WT, gra6-KO, or KO+GRA6 parasites. Relative mRNA levels of *GRA6* compared with the *α-tubulin* level were shown in the y axis. The results of qRT-PCR using primers blue and red were shown in left and right, respectively. Error bars represent means ± SD of triplicates. (J and K) MEFs stably expressing RFP-NFAT4 were infected with WT, gra6-KO, or gra6-KO parasites expressing GRA6 (KO+GRA6) *T. gondii* (moi = 5), fixed at 6 h after infection, and stained with DAPI. Bars, 5 µm. The representative images are shown in J and mean nuclear RFP signal was measured in K. The y axis represents the mean nuclear RFP signal (NFAT4) intensity over all the cells. *, $P < 0.001$ (WT vs. gra6-KO); **, $P < 0.001$ (gra6-KO vs. KO+GRA6), determined by unpaired Student's *t* test. Data are representative of three (A) and two (C–G and I–K) independent experiments.

Published September 15, 2014

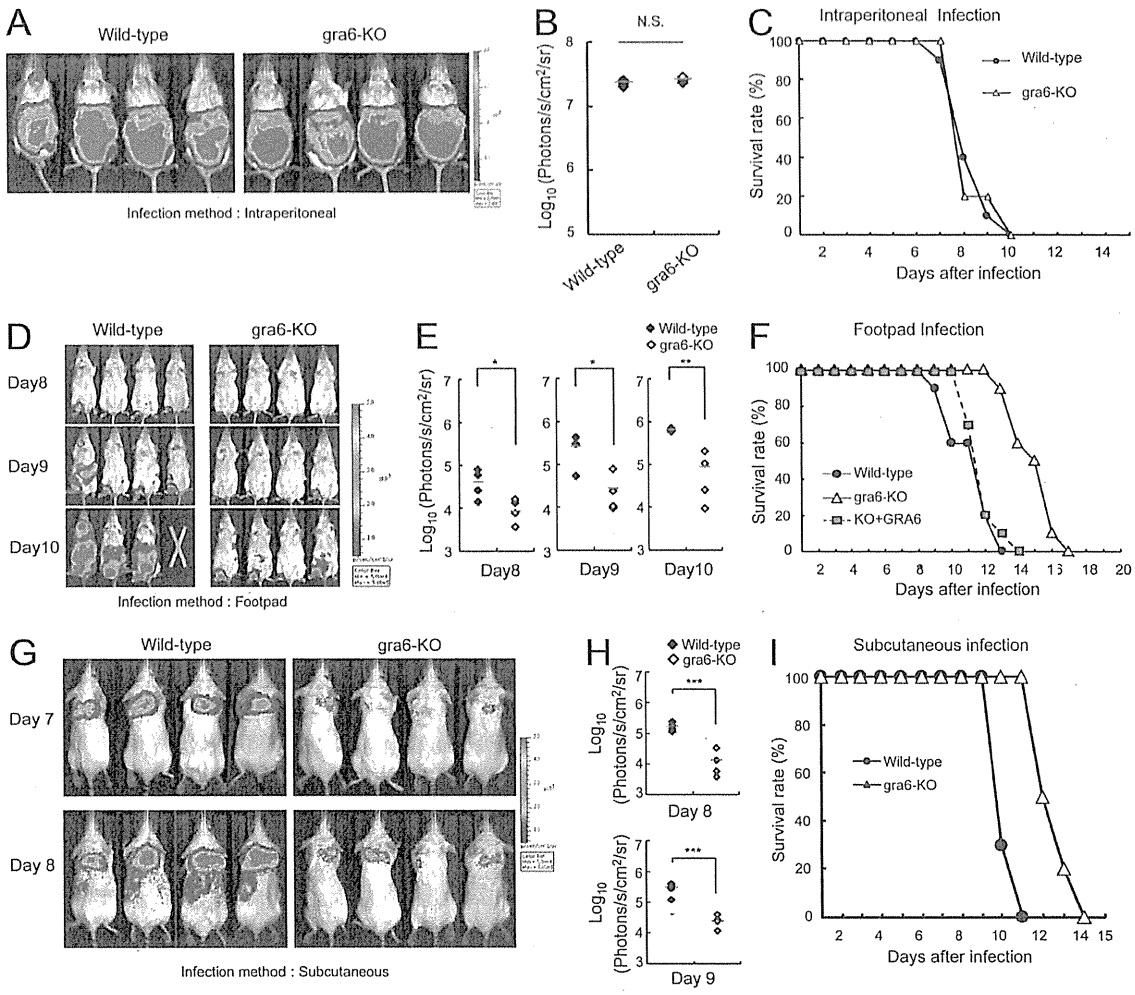

Figure 5. GRA6 is required for *T. gondii* local infection-mediated full virulence. (A and G) BALB/c mice (n = 4 per each group) were intraperitoneally (A) or subcutaneously (G) infected with 10^3 WT or gra6-KO luciferase-expressing parasites, and the progress of infection was assessed by BLI at 6 d (A) or indicated days (G) after infection. The color scales indicate photon emission during a 60-s exposure. (B and H) Total photon emission analysis from BALB/c mice (n = 4 per each group) in A or G. Abdominal photon emission was assessed during a 60-s exposure. (C and I) BALB/c mice (n = 10 per each group) were intraperitoneally (C) or subcutaneously (I) infected with 10^3 WT or gra6-KO parasites, and the survival rates monitored for 15 d. $P < 0.001$ (subcutaneous infection, significant; WT vs. gra6-KO, log-rank test). (D) BALB/c mice (n = 4 per each group) were infected into right footpads with 10^3 WT or gra6-KO luciferase-expressing parasites, and the progress of infection was assessed by BLI at indicated days after infection. The color scales indicate photon emission during a 60 s exposure. (E) Total photon emission analysis from mice (n = 4) in D. Abdominal photon emission was assessed during a 60-s exposure. (F) BALB/c mice (n = 10 per each group) were infected into right footpads with 10^3 WT, gra6-KO, or KO+GRA6 parasites, and the survival rates monitored for 20 d. $P < 0.001$: WT vs. gra6-KO, log-rank test; $P < 0.001$: gra6-KO vs. KO+GRA6, log-rank test. *, $P < 0.05$; **, $P < 0.005$; ***, $P < 0.01$; N.S., nonsignificant, determined by unpaired Student's t test in B, E, and H. The red bars show means of the four (or three for WT of day 10) samples (B, E, and H). Data are representative of three (D and E) or two (A, B, G, and H) independent experiments or cumulative percentages of two independent experiments (C, F, and I).

to generate homozygotic mice of the mutated allele. Fibroblasts of the homozygotic mice were tested for the NFAT4 protein expression by Western blotting and found to contain no NFAT4 proteins (Fig. 8 B), confirming the successful generation of *NFAT4*-deficient mice by the genome editing method.

Then we assessed the induction of mRNAs for *Cxcl2* and *Cd2* in response to WT parasite infection in fibroblasts (Fig. 8 C). Compared with WT cells, *T. gondii* infection-mediated expression of both chemokines was significantly impaired in *NFAT4*-deficient cells (Fig. 8 C). Next, we compared recruitment of $CD11b^+$ $Ly6G^+$ cells in the footpad of WT or *NFAT4*-deficient mice infected with WT parasites (Fig. 8, D–F). At day 5 after infection of WT parasite, the footpads in WT mice included higher frequencies and numbers of $CD11b^+$ $Ly6G^+$ cells than those in *NFAT4*-deficient mice

Published September 15, 2014

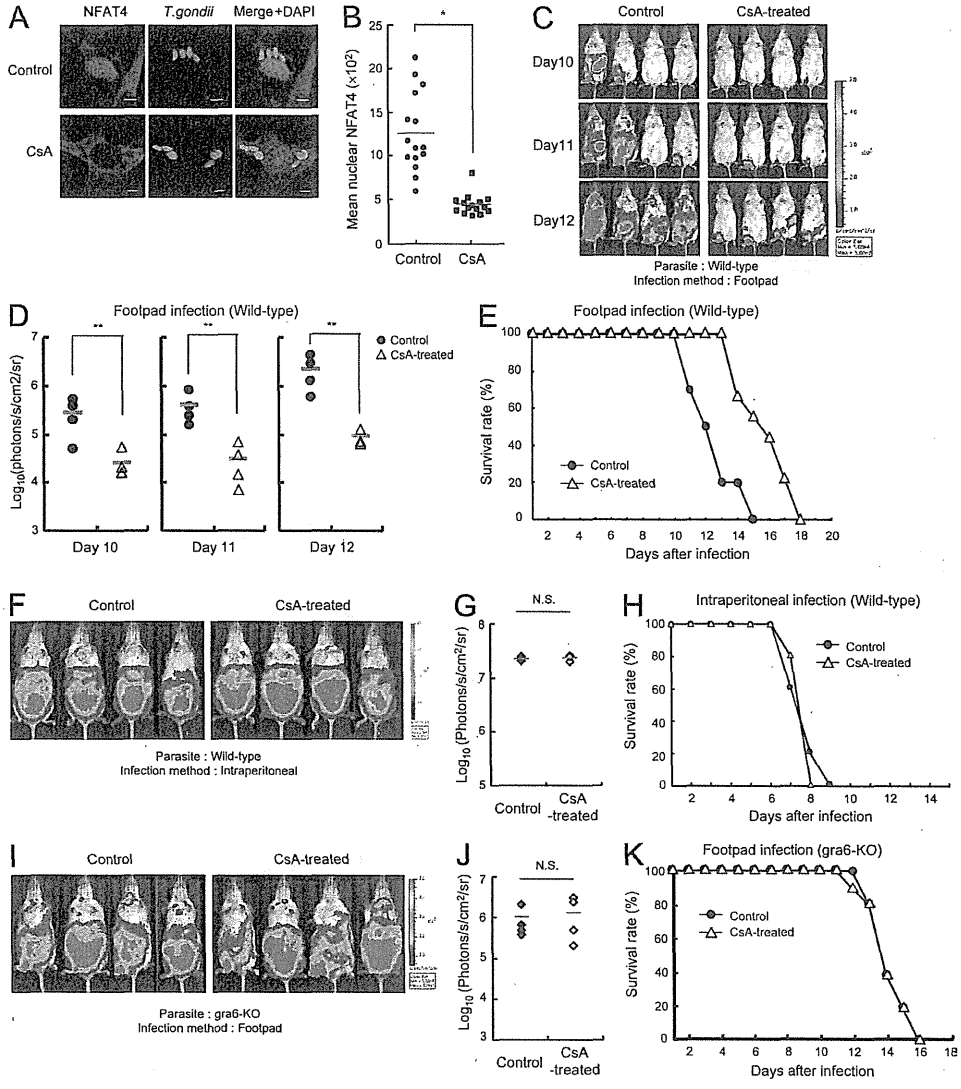

Figure 6. CsA treatment inhibits virulence by the local infection of WT, but not *GRA6*-deficient, parasites. (A and B) MEFs stably expressing RFP-NFAT4 were infected with WT RH *T. gondii* (moi = 5) in the presence or absence of 100 ng/ml CsA or DMSO, fixed at 6 h after infection, and stained with DAPI. Bars, 5 µm. The representative images are shown in A and mean nuclear RFP signal was measured in B. The y axis represents the mean nuclear RFP signal (NFAT4) intensity over all the cells. (C) BALB/c mice ($n = 4$ per each group) treated with 30 mg/kg CsA or the vehicle alone (control) were infected into right footpads with 10^3 WT luciferase-expressing parasites, and the progress of infection was assessed by BLI at indicated days after infection. The color scales indicate photon emission during a 60-s exposure. (D) Total photon emission analysis from mice ($n = 4$ per each group) in C. Abdominal photon emission was assessed during a 60-s exposure. (E) BALB/c mice treated with CsA ($n = 9$) or the vehicle alone ($n = 10$) were infected into right footpads with 10^3 WT parasites, and the survival rates monitored for 20 d. $P < 0.001$ (CsA-treated vs. control, log-rank test). (F and I) Control or CsA-treated BALB/c mice ($n = 4$ per each group) were intraperitoneally infected with 10^3 WT luciferase-expressing parasites (F), or infected into right footpads with 10^3 gra6-KO luciferase-expressing parasites (I), and the progress of infection was assessed by BLI at 7 d (F) or 11 d (I) after infection. The color scales indicate photon emission during a 60-s exposure. (G and J) Total photon emission analysis from control or CsA-treated BALB/c mice ($n = 4$ per each group) in F or I. Abdominal photon emission was assessed during a 60-s exposure. N.S., nonsignificant. (H and K) Survival rates ($n = 10$ per each group) were monitored for indicated days for mice in F or I. *, $P < 0.001$; **, $P < 0.05$; N.S., nonsignificant, determined by unpaired Student's *t* test in B, D, G, or J. The red bars show means of the four samples (D, G, and J). Data are representative of two independent experiments (A–G, I, and J) or cumulative percentages of two independent (E, H, and K) experiments.

(Fig. 8, D–F), indicating that *T. gondii* infection mediates the local induction of Cxcl2 and Ccl2, and causes $CD11b^+$ $Ly6G^+$ cell recruitment in an *NFAT4*-dependent fashion. To test whether NFAT4 is required for the full virulence by the local infection of *T. gondii*, WT or *NFAT4*-deficient mice were locally infected with WT parasite and analyzed the parasite

Published September 15, 2014

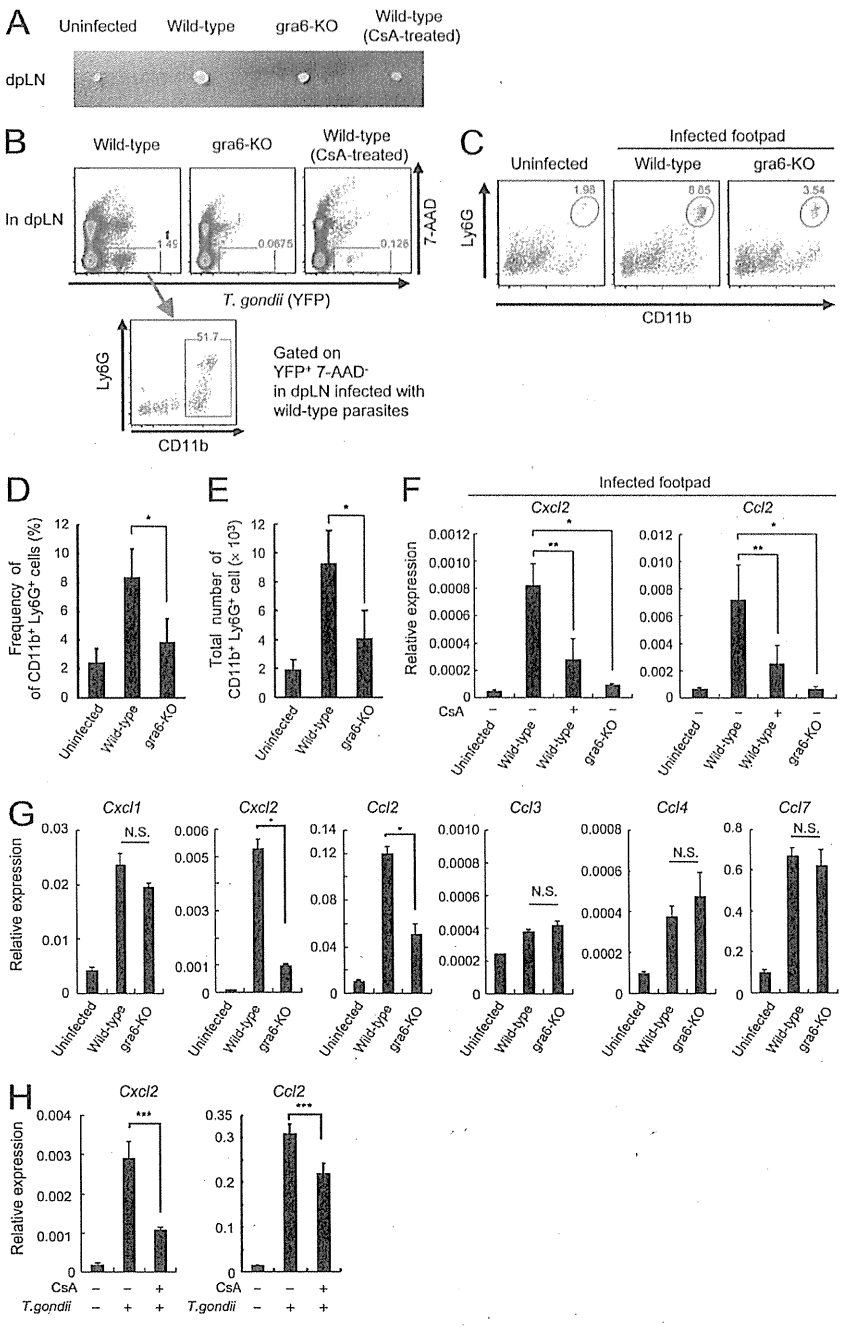

Figure 7. GRA6-dependent recruitment of CD11b⁺ Ly6G⁺ cells to the infected footpad and induction of chemokines. (A) dpLN in control or CsA-treated BALB/c mice infected into right footpads with WT or gra6-KO parasites expressing YFP at day 5 after infection. (B) Flow cytometric analysis showing the cell population contained in the dpLNs of indicated mice. Single cell suspensions from each dLN were gated on live (7-AAD⁻) and *T. gondii*–positive (YFP⁺) population (top). YFP⁺ populations in dpLN of mice infected with WT parasites were analyzed with Ly6G and CD11b. The percentage of CD11b⁺ population was shown (bottom). (C) Representative flow cytometric plots of single cell suspension from the footpads of indicated mice at day 4 after infection. Single cell suspension was stained with 7-AAD and CD45.2. Then CD45⁺ and 7-AAD⁻ populations were analyzed with Ly6G and CD11b. The percentages of CD11b⁺ Ly6G⁺ cells were shown. (D and E) Frequencies (D) and total numbers (E) of CD11b⁺ Ly6G⁺ cells of uninfected footpads ($n = 5$) or ones infected with WT ($n = 5$) or gra6-KO ($n = 4$) parasites. Indicated values represent means ± SD of all samples of each group. (F) Quantitative RT-PCR analysis was performed using cDNA reversely transcribed from RNA extracted from footpads of uninfected mice or ones infected with WT or gra6-KO parasites, and CsA-treated mice ($n = 3$ per group) at day 7 after infection. Indicated values represent means ± SD of triplicates. (G and H) Quantitative RT-PCR analysis was performed using cDNA reversely transcribed from RNA extracted from tail fibroblasts infected with WT or gra6-KO parasites (moi = 5; G) or WT parasite-infected (moi = 5) tail fibroblasts untreated or treated with 100 ng/ml CsA (H). Relative mRNA levels of indicated genes compared with the *GAPDH* level were shown in the y axis. Indicated values represent means ± SD of triplicates. *, $P < 0.01$; **, $P < 0.04$; ***, $P < 0.03$; N.S., nonsignificant, determined by unpaired Student's *t* test in D–H. Data are representative of two (A, B, and F–H) or three (C–E) independent experiments.

spread by the in vivo imaging. Reminiscent of mice infected with *GRA6*-deficient parasites or CsA-treated mice infected with WT parasites, *NFAT4*-deficient mice challenged with WT parasites exhibited significantly delayed parasite translocation in comparison with WT mice (Fig. 8, G and H). Moreover, survival of *NFAT4*-deficient mice infected with WT parasites was markedly prolonged compared with that of WT mice (Fig. 8 I). Thus, these results indicate that NFAT4 plays a vital role in the full virulence by the local infection of WT *T. gondii*.

Strain-dependent NFAT4 activation by GRA6

The *GRA6* gene is highly polymorphic and has been a good genetic marker for strain characterization and genotyping of field and clinical isolates of *T. gondii* (Fazaeli et al., 2000). The amino acid sequence of type II GRA6 contains amino acid

Published September 15, 2014

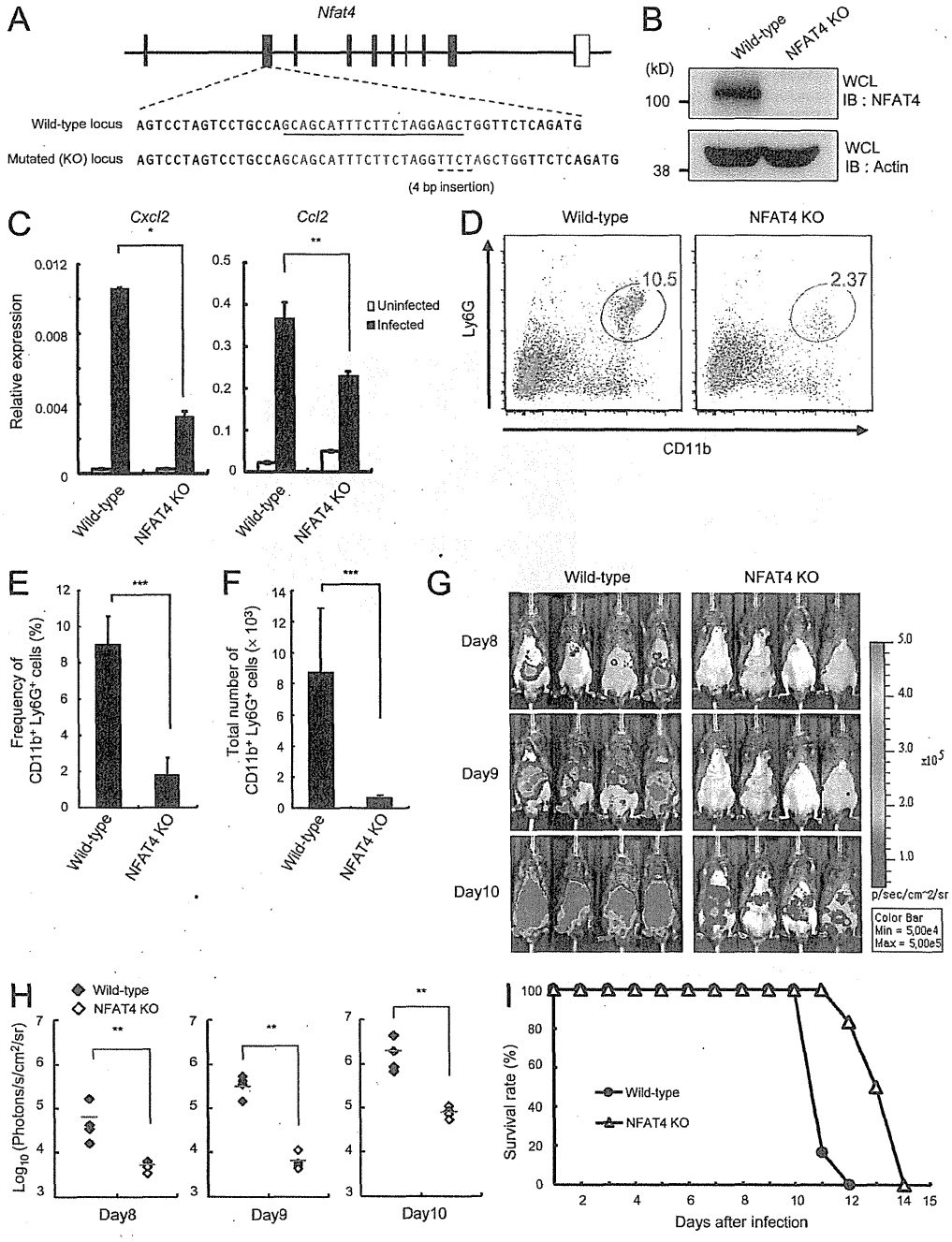

Figure 8. NFAT4 is required for full virulence by WT parasites. (A) Schematic of the Cas9/gRNA-targeting site in the second of *Nfat4* gene. Top: Structure of the *Nfat4* gene. Black and white boxes denote the coding and noncoding exons, respectively. Middle: The target sequence for gRNA (underlined) and the PAM sequence were labeled with green and red, respectively. Bottom: The sequence of the mutated allele contained an insertion of 4 bp (dashed underlined and labeled with brown), resulting in a frameshift mutation. (B) Lysates of tail fibroblasts from indicated mice were subjected to Western blot with indicated Abs. (C) Quantitative RT-PCR analysis was performed using cDNA reversely transcribed from RNA extracted from WT parasite-infected (moi = 5) tail fibroblasts derived from WT or *NFAT4*-deficient mice. Relative mRNA levels of indicated genes compared with the *GAPDH* level were shown in the y axis. Indicated values represent means ± SD of triplicates. (D) Representative flow cytometric plots of single cell suspension from the foot-pad of WT or *NFAT4*-deficient mice at day 5 after infection of WT parasites was stained with 7-AAD and CD45.2. Then $CD45^+$ and $7\text{-}AAD^-$ populations were analyzed with Ly6G and CD11b. The percentages of $CD11b^+$ $Ly6G^+$ cells were shown. (E and F) Frequencies (E) and total numbers (F) of $CD11b^+$ $Ly6G^+$ cells of WT ($n = 4$) or *NFAT4*-deficient ($n = 3$) mice infected with WT parasites at day 5 after infection. Indicated values represent means ± SD of all samples

Published September 15, 2014

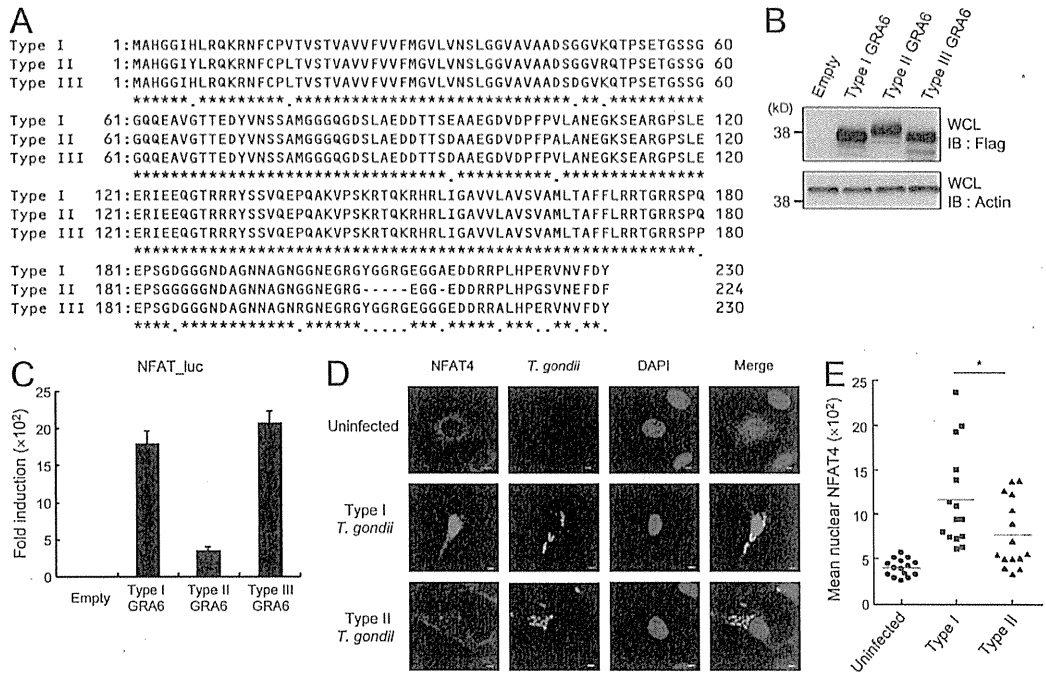

Figure 9. GRA6-mediated NFAT4 activation is strain-dependent. (A) The predicted amino acid sequence for the primary translation product of the *GRA6* gene is shown for type I parasites on the top line. The sequences for type II and type III parasites are shown on the second and third line with a dash to indicate identity to the all strains sequence, respectively. (B) Lysates of 293T cells transfected with indicated expression vectors were subjected to Western blotting. (C) 293T cells were transfected with the NFAT-luc plasmid together with the indicated GRA6 expression vectors. Luciferase activities were expressed as indicated above. Error bars represent means ± SD of triplicates. (D and E) MEFs stably expressing RFP-NFAT4 were uninfected or infected with type I or type II *T. gondii* (moi = 5), fixed at 6 h after infection, and stained with DAPI. Bars, 5 µm. The representative images are shown in D and mean nuclear RFP signal was measured in E. The y axis represents the mean nuclear RFP signal (NFAT4) intensity over all the cells. *, $P < 0.03$, determined by unpaired Student's *t* test in E. Data are representative of three (B and C) and two (D and E) independent experiments.

substitutions and deletions compared with the sequences of type I and III GRA6 (Fig. 9 A). To examine whether this strain difference in GRA6 affects NFAT4 activation, we cloned type II and type III GRA6 cDNAs into mammalian expression vectors and tested the activity of the NFAT-dependent promoter using a luciferase assay. Although ectopic expression of type I and type III GRA6 yielded comparable activation of the NFAT-dependent reporter, the degree of type II GRA6-mediated activation was less, despite similar protein expression levels (Fig. 9, B and C). We next assessed whether the degree of NFAT4 activation after infection with type I or type II parasites was different. Compared with infection with type I parasites, infection with type II parasites resulted in markedly less nuclear translocation of NFAT4 (Fig. 9, D and E), indicating strain-dependent NFAT4 activation by GRA6.

The C-terminal polymorphisms on GRA6 determine the strain-dependent NFAT4 activation

Finally, we analyzed which regions of the type II GRA6 protein are responsible for the defective NFAT4 activation. The N-terminal and C-terminal domains of GRA6 were swapped between type I and type II GRA6, and tested for the potency of NFAT4-dependent activation using a luciferase assay. A chimeric GRA6 harboring the C terminus of type II GRA6 failed to activate the NFAT-dependent promoter (Fig. 10 A). This region contains five amino acid substitutions (Fig. 9 A). Each of the substitutions in the very C terminus of type I

of each group. (G) WT or *NFAT4*-deficient mice ($n = 4$ per each group) were infected into right footpads with 10^3 WT luciferase-expressing parasites, and the progress of infection was assessed by BLI at indicated days after infection. The color scales indicate photon emission during a 60-s exposure. (H) Total photon emission analysis from WT or *NFAT4*-deficient mice ($n = 4$ per each group) in G. Abdominal photon emission was assessed during a 60-s exposure. The red bars show means of the four samples. (I) Survival rates ($n = 6$ per each group) were monitored for 15 d for mice in G. $P < 0.002$ (WT vs. *NFAT4*-deficient mice, log-rank test). *, $P < 0.001$; **, $P < 0.05$; ***, $P < 0.01$; N.S., nonsignificant, determined by unpaired Student's *t* test in C, E, F, and H. Data are representative of two (B and D–H) or three (C) independent experiments or cumulative percentages of two independent (I) experiments.

Published September 15, 2014

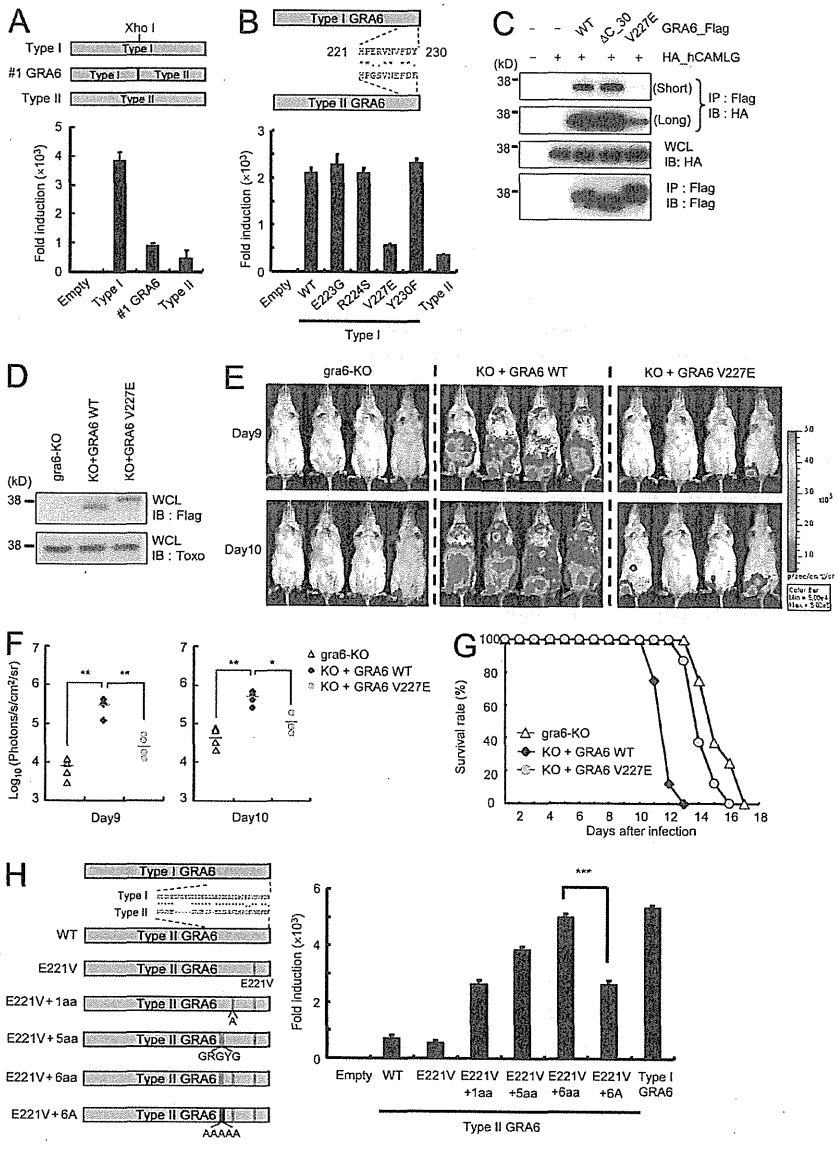

Figure 10. Polymorphisms on the C terminus determine the strain-specific NFAT4 activation and local infection-induced virulence. (A and B) 293T cells were transfected with the NFAT-luc plasmid, together with the indicated GRA6 expression vectors. Luciferase activities were expressed as indicated above. Error bars represent means ± SD of triplicates. A list of the point mutants of GRA6 expression vectors is shown (A and B, top). Type I, red; Type II, blue. (C) Lysates of 293T cells transiently cotransfected with Flag-tagged type I GRA6 variants and/or HA-tagged CAMLG were immunoprecipitated with the indicated Abs and subjected to Western blotting. Short and long indicate the time of exposure. (D) Lysates of indicated parasites were subjected to Western blotting using indicated Abs. (E) BALB/c mice (n = 4 per each group) were infected into right footpads with 10^3 gra6-KO (parental line), KO+GRA6 WT, or KO+GRA6 V227E luciferase-expressing parasites, and the progress of infection was assessed by BLI at indicated days after infection. The color scales indicate photon emission during a 60-s exposure. (F) Total photon emission analysis from BALB/c mice (n = 4) in E at indicated days after infection. Abdominal photon emission was assessed during a 60-s exposure. The red bars show means of the four samples. (G) The survival rates for mice in E (n = 8 per each group) were monitored for 18 d. $P < 0.001$ (significant; KO+GRA6 WT vs. KO+GRA6 V227E, log-rank test). $P > 0.05$ (nonsignificant; gra6-KO vs. KO+GRA6 V227E, log-rank test). (H) 293T cells were transfected with the NFAT-luc plasmid together with the indicated GRA6 expression vectors. Luciferase activities were expressed as indicated above. Error bars represent means ± SD of triplicates. A list of the point mutants of GRA6 expression vectors is shown (H, left). *, $P < 0.03$; **, $P < 0.01$; ***, $P < 0.001$, determined by unpaired Student's t test in F or H. Data are representative of three (A, B, and H) or two (C–F) independent experiments or cumulative percentages of two independent experiments (G).

GRA6 was replaced with the corresponding sequence in type II GRA6, and the chimeras were tested for NFAT-dependent reporter activation. Among them, the substitution of a valine residue at position 227 to a glutamic acid residue (V227E) culminated in a remarkable decrease in NFAT activation to a level comparable to that mediated by type II GRA6 (Fig. 10 B). We next compared interaction of WT, ΔC_30, or V227E type I GRA6 with HA-CAMLG by coimmunoprecipitation assay (Fig. 10 C). We found that V227E type I GRA6 coprecipitated with HA-CAMLG to a markedly lesser degree than the WT or ΔC_30 form did (Fig. 10 C). To assess whether the V227E substitution in type I GRA6 affects virulence by local infection, BALB/c mice were infected with *GRA6*-deficient parasites expressing WT or V227E type I GRA6 at similar levels (Fig. 10 D). Compared with WT GRA6-expressing parasites, *GRA6*-deficient parasites complemented with the V227E exhibited significantly delayed spreading and mortality (Fig. 10, E–G), indicating that impaired NFAT4 activation, probably due to the inefficient CAMLG–GRA6 interaction by the V227E substitution, may result in the defective virulence in the local infection. Lastly, we examined whether the single reverse mutation of the glutamic acid at position 221 to

Published September 15, 2014

a valine (E221V) in type II GRA6 could restore NFAT activation. However, the reverse E221V mutation in type II GRA6 failed to restore NFAT activation (Fig. 10 H), suggesting that the reverse mutation may be insufficient for the restoration of type II GRA6.The C terminus of type II GRA6 also contains six amino acid deletions (Fig. 9 A). Therefore, we added one (+1aa), five (+5aa), and six (+6aa) amino acids contained in type I GRA6 to the E221V mutant of type II GRA6, and tested for NFAT activation. We found that full restoration was achieved only if all six amino acids were added to the E221V mutant of type II GRA6 (Fig. 10 H). Furthermore, when all five of the amino acids added to type II GRA6 were replaced with alanines, NFAT activation induced by the E221V mutant of type II GRA6 (+6A) was diminished to a level similar to that induced by the +1aa mutant of type II GRA6 (Fig. 10 H). These results demonstrated that the C-terminal residue V227 in type I GRA6 (E221 in type II GRA6) and the deletion of six other amino acids are the determinants of strain-dependent NFAT4 activation.

DISCUSSION

In the present study, we demonstrated that a *T. gondii* dense granule protein GRA6 robustly activates the host transcription factor NFAT4 via CAMLG. GRA6 was originally identified as a dense granule protein that plays an important role in the stabilization of the membranous nanotubular network (MNN) in *T. gondii* PVs (Mercier et al., 2002). The network is considered to increase the surface area of the interface between parasites and the host cytoplasm (Sibley et al., 1995; Mercier et al., 2002; Reese and Boothroyd, 2009). Although the N terminus of GRA6 is required for targeting the protein to the MNN, the C terminus and/or transmembrane domain determines the topology (Gendrin et al., 2010). Considering that a fusion protein harboring the N terminus of GRA5 and the transmembrane domain and C terminus of GRA6 was located in the PVM with the C terminus topologically facing the host cytoplasm (Gendrin et al., 2010), together with our findings, the C terminus of GRA6 might interact with CAMLG on the host cytoplasmic side of the MNN. Although CAMLG is reportedly an NFAT activator (Bram and Crabtree, 1994), whether this molecule broadly or selectively activates NFAT proteins remains to be seen. Our present results demonstrate strong synergistic activation of the NFAT-dependent promoter in cells coexpressing CAMLG and NFAT4, and specific association of CAMLG with NFAT4 and GRA6 but not with other NFAT members. In addition, a part of CAMLG is shown to be colocalized with PVMs in *T. gondii*–infected cells (Kim et al., 2008), presumably reflecting PV recruitment of host ERs, where CAMLG resides (Yamamoto and Sakisaka, 2012). Given that CAMLG activates calcineurin by causing intracellular calcium influx (Bram and Crabtree, 1994), GRA6 interaction with CAMLG in MNNs, where PVMs and host ER membranes can be encountered, might induce very local activation of calcineurin by regulating calcium influx from host ERs, resulting in subsequent activation of NFAT4 associating with CAMLG at the site.

We found that *GRA6*-deficient type I parasites fail to show full virulence when locally infected into the footpads or subcutaneous tissues of mice, whereas systemic infection into the peritoneal cavity resulted in virulence comparable to that of WT parasites. Unlike intraperitoneal infection, which results in acute systemic infection soon after inoculation, the footpad local infection in this study might allow us to observe the gradual and time-dependent in vivo spreading of *T. gondii*. Knockout type I parasites with no significant in vivo difference from WT parasites in the systemic intraperitoneal infection paradigm might produce a phenotype in mice locally infected into footpads, eyes, or subcutaneous tissues (Hu et al., 1999).

NFAT4 was initially shown to play a role in the homeostasis of T cells (Oukka et al., 1998), but a growing amount of evidence has revealed that NFAT4 is expressed in many cell types and functions in a variety of physiological and pathological processes such as tissue regeneration, pulmonary hypertension, and development of heart and muscle (Bushdid et al., 2003; Pierre et al., 2009; Bierer et al., 2011). In the present study, we have demonstrated the specific function of NFAT4 activation in induction of Cxcl2 and Ccl2 mRNAs at cellular/tissue levels and $CD11b^+$ $Ly6G^+$ cell recruitment to the infected footpad. Cxcl2 and Ccl2 are chemokines that play pivotal roles of recruitment of $CD11b^+$ cells such as neutrophils and inflammatory monocytes (Appelberg, 1992; Lu et al., 1998). In contrast to the modest defect in Ccl2 induction that is regulated mainly by NF-κB or AP-1 (Martin et al., 1997; Ruiz-Ortega et al., 2000), the impairment in Cxcl2 induction was more profound in NFAT4-deficient cells or CsA-treated cells. Collectively, the GRA6-NFAT4–dependent induction of Cxcl2 rather than Ccl2 may be important for the $CD11b^+$ $Ly6G^+$ cell recruitment to the infected site. Similarly, a recent study in acute pancreatic mouse model reveals that NFAT4 is involved in pancreatic Cxcl2 expression and $Ly6G^+$ cell infiltration (Awla et al., 2012), suggesting the universal role of NFAT4 in Cxcl2 induction and $CD11b^+$ $Ly6G^+$ cell recruitment. In terms of the parasite spread, $CD11b^+$ cells, including macrophages, monocytes, neutrophils, and dendritic cells, are exploited for the systemic dissemination from the infected site (Courret et al., 2006; Bierly et al., 2008; Coombes et al., 2013). Moreover, we have demonstrated that dpLNs from mice infected with WT *T. gondii* had parasite-containing $CD11b^+$ $Ly6G^+$ cells. After the cell population is recruited to the infected footpad in the GRA6/NFAT4-dependent manner, the $CD11b^+$ $Ly6G^+$ cells might at some point be locally infected with *T. gondii*, migrate to dpLNs, and eventually disseminate into the whole body. Indeed, $CD11b^+$ $Ly6G^+$ cells (neutrophils) are recently shown to be nonprotective during acute infection with *T. gondii* in vivo (Dunay et al., 2010) and to play an important role in the spread of infection as a highly motile *T. gondii* carrier in the oral infection model (Coombes et al., 2013). Furthermore, a new family member of GRA proteins, GRA25, has been newly identified as a virulence factor that modulates production of chemokines such as Ccl2 and Cxcl1 in type II *T. gondii* (Shastri et al., 2014). Although the molecular mechanism by

Published September 15, 2014

which GRA25 influences host cellular signaling pathways that lead to production of these chemokines remains uncertain, given less GRA6-dependent NFAT4 activity in type II *T. gondii*, GRA25 in place of GRA6 might play a role in production of chemokines, promotion of $CD11b^+$ cell recruitment, and the parasite spread for type II parasites.

Because the *GRA6* gene is highly polymorphic and singly encoded in the *T. gondii* genome, this locus, in addition to the loci of other polymorphic genes such as *SAG2*, *SAG3*, *BTUB*, and *PK1*, is often tested by multilocus PCR restriction fragment length polymorphism analysis when genotyping field and clinical isolates of *T. gondii* (Su et al., 2006). In particular, the C terminus contains not only nucleotide substitutions but also two deletions of 15 and 3 bp in the *GRA6* gene, resulting in six amino acid deletions. Furthermore, the deletions are suggested to be linked to avirulence in exotic lines (Fazaeli et al., 2000). In this study, we have demonstrated the role of the C-terminal six amino acids, in addition to E221V substitution, in fully restoring type II GRA6-mediated NFAT4 activation. Considering that *GRA6*-deficient parasites complemented with V227E type I GRA6 possessing lower potency for NFAT4 activation failed to restore the virulence (Fig. 10) and that the reduction in the virulence of WT parasites was achieved by biochemical transient or genetic constitutive inactivation of NFAT4 in mice by the CsA treatment or the Cas9/CRISPR-mediated genome editing, respectively (Figs. 6 and 8), NFAT4 plays a major role in the GRA6-dependent parasite virulence program. Treatment using high levels of CsA has been reported to inhibit parasite invasion and replication (Mack and McLeod, 1984; McCabe et al., 1986). However, because the CsA concentration in this study did not inhibit spread and virulence induced by the systemic infection of WT parasites or the local infection of *GRA6*-deficient parasites (Fig. 6), the effect of CsA treatment on the reduced virulence after local infection may be dependent on the presence of GRA6 but independent of the direct antiparasitic activity of CsA on invasion and replication. Further studies to reveal the relationships among polymorphisms in the C terminus of GRA6, NFAT4 activity, and virulence in mice systemically or locally infected with nonarchetypal *T. gondii* lines would be of interest. However, the C terminus of GRA6 contains an important T cell epitope that is involved in induction of low or high CD8 T cell responses by infection with avirulent parasites expressing type I/III or type II GRA6, respectively (Blanchard et al., 2008; Feliu et al., 2013). Therefore, one should be cautious because an attempt to generate type II parasites with higher NFAT4 activity in the infection by replacing the GRA6 to the type I/III ones might affect the CD8T cell response by removing the highly immunodominant T cell epitope.

The C-terminal 30 amino acid extension of type I GRA6 is not essential for the interaction of CAMLG and NFAT4 activation (Fig. 2). However, both are markedly impaired by the V227E substitution in type I GRA6 (Fig. 10). The V227E substitution in type I GRA6 that is expressed in both mammalian cells and parasites results in slow migration of this protein in SDS-PAGE (Fig. 10, C and D). Notably, the slowly migrated form of GRA6 is also observed in type II GRA6 produced in mammalian cells or parasites, whereas the molecular weight of type II GRA6 is predicted to be lower than that of type I GRA6 (Fig. 9 B; Feliu et al., 2013), indicating that the glutamic acid in the C-terminal position plays an important role in modification of the original type I GRA6 into this slowly migrated form. Although the kind of protein modification and the molecular mechanism by which the V227E substitution triggers the modification are currently unknown, the slowly migrated form of GRA6 may no longer associate with CAMLG and subsequently activate NFAT4 as efficiently as WT type I GRA6 or the ΔC_30 form, both of which are not modified due to the lack of the key glutamic acid. Alternatively, given that the V227E substitution is the dramatic change of amino acids in terms of polarity and electric charge, the amino acid change in the nonessential C-terminal portion of GRA6 might possibly and unexpectedly disturb the CAMLG association with the essential C-terminal CAMLG binding regions of GRA6 by affecting either CAMLG or itself, leading to the reduced association between GRA6 and CAMLG.

In summary, this study highlights a novel virulence program operated by *T. gondii* GRA6 that is required for the selective NFAT4 activation, the manipulation of host immune responses, and the parasite dissemination in a strain-dependent manner. Like *T. gondii* ROPs and GRAs, it is speculated that effector molecules secreted from other intracellular parasites, such as *Plasmodium*, *Leishmania*, and *Trypanosoma*, are involved in subverting and co-opting host gene expression by activating or inactivating host signal transduction (Hiller et al., 2004; Unnikrishnan and Burleigh, 2004; Marti et al., 2005; Silverman et al., 2008). Future studies with the help of an initial in vitro reporter screening may provide us with a better understanding of the host–parasite interface.

MATERIALS AND METHODS

Cells, mice, and parasites. 6–8-wk-old BALB/c mice were obtained from SLC. All animal experiments were conducted with the approval of the Animal Research Committee of Research Institute for Microbial Diseases in Osaka University. ME49, RHΔhxgprtΔku80 and its derivatives of *T. gondii* were maintained in Vero cells by biweekly passage in RPMI (Nacalai Tesque) supplemented with 2% heat-inactivated FCS (JRH Bioscience), 100 U/ml penicillin, and 0.1 mg/ml streptomycin (Nacalai Tesque). 293T cells and fibroblasts were maintained in DMEM (Nacalai Tesque) containing 10% heat-inactivated FCS and antibiotics.

Reagents. Antibodies against CAMLG, NFAT2, NFAT4, HA-probe, and anti-Actin were from Santa Cruz Biotechnology, Inc. Anti-Flag, PMA, and calcium ionophore (A23187) were obtained from Sigma-Aldrich. CsA was obtained from TCI America.

Mammalian expression plasmids. To construct the mammalian expression vectors for GRAs, we deleted regions of signal peptide of individual GRAs when they were predicted in ToxoDB (Fig. 1 A). For GRA15, cDNA encoding amino acids 51–550 was included in the expression vector (Rosowski et al., 2011). cDNA fragments for GRA proteins were amplified using primer sets (Fig. S1): GRA1_F and GRA1_R for GRA1; GRA2_F and GRA2_R for GRA2; GRA3_F and GRA3_R for GRA3; GRA4_F and GRA4_R for GRA4; GRA5_F and GRA5_R for GRA5; GRA1_F

Published September 15, 2014

and GRA6_R for GRA6; GRA7_F and GRA7_R for GRA7; GRA8_F and GRA8_R for GRA8; GRA9_F and GRA9_R for GRA9; GRA10_F and GRA10_R for GRA10; GRA12_F and GRA12_R for GRA12; GRA14_F and GRA14_R for GRA14; and GRA15_F and GRA15_R for GRA15 using RH strain (type I) or ME49 (type II) cDNA as the template and then ligated into the EcoRI–XhoI or BamHI–XhoI sites of a pcDNA vector for the C-terminal Flag-tagged proteins (Invitrogen). cDNAs for GRA7 (BamHI–NotI) and GRA10 (BglII–NotI) were inserted into the BamHI–NotI site of pcDNA vector for the N-terminal Flag-tagged proteins. The series of type I GRA6 fragments containing point or deletion mutations were generated using the following primers: rhGRA6 ΔC30_R for ΔC30; rhGRA6 ΔC60_R for ΔC60; rhGRA6_#1_R for E223G; rhGRA6_#2_R for R224S; rhGRA6_#3_R for V227E; and rhGRA6_#4_R for Y230F and GRA6_F primer (Fig. S1). The series of type II GRA6 mutants containing point mutations were generated using the following primers: meGRA6_R for full-length type II GRA6; meGRA6_R for WT type II GRA6; meGRA6_#1_R for V221E; meGRA6_#2_R for E221E+1aa; and meGRA6_#3_R for V221E+5aa and meGRA6_F primer. The fragments for type II GRA6 E221V+6aa or E221V+6A were generated using the following primers: meGRA_#2_R and meGRA6_F using E221V+5aa or the PCR fragment amplified using meGRA6_F and meGRA6_#4_R as the template, respectively. cDNA for murine NFAT isoforms were amplified using primer sets (Fig. S1): NFAT1_F and NFAT1_R for NFAT1; NFAT2_F and NFAT2_R for NFAT2; NFAT3_F and NFAT3_R for NFAT3; and NFAT4_F and NFAT4_R for NFAT4 using murine cDNA as the template and then ligated into the EcoRI–XhoI or BamHI–XhoI sites of a pcDNA vector for the C-terminal Flag-tagged proteins. Human CAMLG cDNA was amplified using the following primer sets: hCAMLG_F and hCAMLG_R for full-length hCAMLG; and hCAMLG_F and hCAMLG_DN_R for hCAMLG dominant-negative using human cDNA as the template and then ligated into the BamHI–NotI sites of a pcDNA vector for the N-terminal HA-tagged proteins. The sequences of all constructs were confirmed by sequencing using ABI PRISM Genetic Analyzer 3130 (Applied Biosystems).

Generation of RHΔhxgprtΔku80 type I *T. gondii* expressing YFP and luciferase. To express luciferase and YFP in RHΔhxgprtΔku80 *T. gondii*, we transfected pYFPluc plasmids into RHΔhxgprtΔku80 by electroporation (Yamamoto et al., 2012). We selected for RH *T. gondii* parasites stably transfected with pYFPluc with 3 µM pyrimethamine (Sigma-Aldrich) and subjected them to limiting dilution as described previously (Yamamoto et al., 2012). YFP-positive parasites were selected by fluorescent microscopy and tested for in vitro and in vivo luciferase activity. Three clones were isolated, and we observed comparable in vitro growth and in vivo virulence to each other and to the parental line.

Generation of *GRA6*-deficient type I *T. gondii*. Genomic DNA containing the *GRA6* gene was isolated by PCR using primers GRA6KOLA_F and GRA6KOLA_R to generate a 3.3-kb-long fragment. Primers GRA6-KOSA_F and GRA6KOSA_R generated a 1.0 kb fragment (Fig. S1). The gene encoding *T. gondii GRA6* consists of a single exon. The targeting vector (pKO-GRA6) was constructed by replacing the entire coding sequence of *GRA6* with the *HXGPRT* gene expression cassette (p2855). 50 µg of the targeting vector linearized by ScaI were transfected into tachyzoites of the YFPluc RHΔhxgprtΔku80 parasites as previously described (Yamamoto et al., 2009). After 25 µg/ml mycophenolic acid (MPA; Sigma) and 25 µg/ml xanthine (Wako) selection for 14 d, MPA/xanthine-resistant colonies were subjected to limiting dilution to isolate the clones. A total of 48 clones were selected and screened by PCR for detecting homologous recombinants using primers DHFRrc01 (from the DHFR promoter of the *HXGPRT* expression vector) and GRA6ex01 (genomic sequence outside the short fragment of the *GRA6* locus) to detect homologous recombinants. To remove the *HXGPRT* gene expression cassette, we were transiently transfected with RFP-Cre expression vectors. After incubation for 48 h, RFP-positive parasites were sorted using a FACSAriaIII (BD). Then, RFP-positive parasites were subjected to limiting dilution to isolate the clones. A total of 24 clones were selected and screened by PCR for detecting deletion of the *HXGPRT* gene expression cassette using primers GRA6ex01 and GRA6ex02 (from the long fragment of the *GRA6* locus). Subsequently, genomic DNA of WT and *GRA6*-deficient parasites was extracted and subjected to Southern blot analysis using a DNA probe, which was generated by PCR using primers SB_F and SB_R (Fig. S1). In addition, to confirm the disruption of the gene encoding GRA6, we analyzed messenger RNA of *GRA6* from WT and gra6-KO parasites by quantitative RT-PCR.

Generation of transgenic parasites. To complement the *GRA6*-deficient parasites, we generated the C-terminal HA-tagged GRA6 by PCR using TgGRA6_F and TgGRA6HA_R and expressed the GRA6-HA proteins by endogenous promoter containing a *HXGPRT* gene expression cassette in the gra6-KO strain. We generated this vector by inserting the fragment of GRA6-HA into targeting vector (pKO-GRA6). 50 µg of the complementary vector linearized by ScaI were transfected into tachyzoites of the gra6-KOΔhxgprt parasites. We selected for parasites stably expressing the complemented GRA6-HA constructs using 25 µg/ml MPA and 25 µg/ml xanthine selection and subjected these to limiting dilution as described previously (Yamamoto et al., 2009). Furthermore, to confirm the complementation of the GRA6 gene, we analyzed messenger RNA of GRA6 from WT, gra6-KO, and KO+GRA6 parasites by quantitative RT-PCR using primers capable of distinguishing endogenous *GRA6* with that derived from the targeting vector (Fig. S1).

We attempted to introduce the V227E type I GRA6 in the endogenous *GRA6* locus using gra6-KOΔhxgprt for several times but failed by unknown reasons. Therefore, to complement them by overexpression, we first amplified fragments of WT or V227E type I GRA6 by common primers (GRA6_F and pTgGRA6Flag_R) using pGRA6_Flag (for WT) or pTypeI GRA6_V227E, respectively (Fig. S1). The amplified fragments were digested with BamHI and PacI, and cloned into BamHI–PacI site of pS1K_UTR vector possessing the sag1 promoter and UTR (Yamamoto et al., 2011). Then, the NotI fragments containing sag1 promoter-type I GRA6 (WT or V227E)-UTR were ligated into the NotI site of the pHXGPRT vector (p2855), resulting in pTgTypeIGRA6_Flag (WT or V227E). The pTgTypeIGRA6_Flag vectors were individually transfected into tachyzoites of gra6-KOΔhxgprt. We selected transfectants as described above, and obtained several clones with similar expression levels of WT or V227E type I GRA6 (Fig. 10 D).

Generation of stably expressing NFAT4-mCherry and shRNA. To generate MEFs stably expressing mouse NFAT4-mCherry, we constructed a plasmid harboring mouse NFAT4-mCherry fusion protein. NFAT4 fragments were obtained by PCR using the primers mNFAT4_F and mNFAT4_R and murine cDNA as the template (Fig. S1). mCherry fragments were obtained by PCR using the primers mCherry_F and mCherry_R and pmCherry (Takara Bio Inc.) as the template. The EcoRI–XhoI fragment of mNFAT4 and the XhoI–NotI fragment of mCherry were cloned into EcoRI–NotI-digested pMRX-puro retroviral vector. For gene silencing of CAMLG and NFATs, shRNA retroviral vector carrying a target gene sequence for CAMLG, NFAT isoforms, or scrambled shRNA were purchased from Takara Bio Inc. pMRX-puro (mNFAT4-mCherry) retroviral vector and shRNA retroviral vectors were transfected into PLAT-E cells with Lipofectamine 2000 (Invitrogen). At 24 h after transfection, the medium was changed and the cells were cultured for an additional 48 h. The virus-containing supernatants from the PLAT-E cells were harvested and immediately used for infection. At 6 h after infection, the medium was changed with complete growth medium. Cells were selected by the addition of 2 µg/ml puromycin to the culture medium.

Fluorescent microscopic analysis. MEFs stably expressing NFAT4-mCherry were serum starved for 6 h and were infected with *T. gondii* (moi = 5). After incubation for 6 h, cells were fixed for 10 min in PBS containing 3.7% formaldehyde. MEFs stably expressing NFAT4-mCherry were transiently transfected with 2 µg of empty or the C-terminally Flag-tagged

Published September 15, 2014

GRA6 or GRA15 expression vectors using Lipofectamine 2000 (Invitrogen). At 24 h after transfection, cells were fixed. Cells were permeabilized with PBS containing 0.1% Triton X-100 and then blocked with 8% FCS in PBS. Subsequently, cells were incubated with anti-Flag mouse (1:1,000) or anti-GAP45 rabbit antibodies (1:1,000) for 1 h at 37°C, followed by incubation with Alexa Fluor 488–conjugated anti–mouse IgG or Alexa Fluor 488–conjugated anti–rabbit IgG (Invitrogen) for 1 h at room temperature in the dark. Nuclei were counterstained with DAPI (Wako). Finally, the immunostained cells were mounted with PermaFluor (Thermo Fisher Scientific) on glass slides and analyzed by confocal laser microscopy (FV1200; Olympus). The signals of mCherry were directly detected by excitation of the 568 nm laser. The images were analyzed with Fluoview (Olympus).

Quantitative RT-PCR. Total RNA was extracted and cDNA was synthesized using Verso Reverse transcription (Thermo Fisher Scientific). Real-time PCR was performed with a CFX connect real-time PCR system (Bio-Rad Laboratories) using the Go-Taq Real-Time PCR system (Promega). The values were normalized to the amount of glyceraldehyde 3-phosphate dehydrogenase (GAPDH) or α-tubulin in each sample. The following primer sets were used: NFAT1_qpF and NFAT1_qpR for *Nfat1*; NFAT2_qpF and NFAT2_qpR for *Nfat2*; NFAT3_qpF and NFAT3_qpR for *Nfat3*; NFAT4_qpF and NFAT4_qpR for *Nfat4*; Cxcl1_qpF and Cxcl1_qpR for *Cxcl1*; Cxcl2_qpF and Cxcl2_qpR for *Cxcl2*; Ccl2_qpF and Ccl2_qpR for *Ccl2*; Ccl3_qpF and Ccl3_qpR for *Ccl3*; Ccl4_qpF and Ccl4_qpR for *Ccl4*; Ccl7_qpF and Ccl7_qpR for *Ccl7*; GAPDH_qpF and GAPDH_qpR for *GAPDH*; GRA6_qpF and GRA6_qpR for *GRA6*; GRA6HA_qpF and GRA6HA_qpR for GRA6HA; and Tubulin_qpF and Tubulin_qpR for *α-tubulin* (Fig. S1).

Western blot analysis and immunoprecipitation. 293T cells were lysed in a lysis buffer (0.5% Nonidet P-40, 150 mM NaCl, and 20 mM Tris-HCl, pH 7.5) containing a protease inhibitor cocktail (Roche) and phosphatase inhibitor cocktail (Nacalai Tesque). The cell lysates were separated by SDS-PAGE and transferred to polyvinylidene fluoride membranes. For immunoprecipitation, cell lysates were precleared with protein G–Sepharose (GE Healthcare) for 2 h and then incubated with protein G–Sepharose containing 1.0 µg of the indicated antibodies for 12 h with rotation at 4°C. The immunoprecipitants were washed four times with lysis buffer and eluted by boiling with Laemmli sample buffer. The eluates were separated by SDS-PAGE, transferred to polyvinylidene fluoride membranes, and subjected to Western blot analysis as described previously (Yamamoto et al., 2009).

Luciferase assay. PathDetect in Vivo Signal Transduction Pathway cis-Reporting Systems was purchased from Agilent Technologies. The 5× UPRE luciferase reporter was generated as described previously (Yamamoto et al., 2011). The Stat6-dependent TPU reporter was described previously (Mikita et al., 1996). The reporters containing murine IFN-β promoter or harboring NF-κB–dependent ELAM promoter were described previously (Yamamoto et al., 2002). The reporter plasmids were transiently co-transfected into 293T cells with the control *Renilla* luciferase expression vectors using Lipofectamine 2000 reagent (Invitrogen). Luciferase activities of total cell lysates were measured using the Dual-Luciferase Reporter Assay System (Promega) as described previously (Yamamoto et al., 2009).

CsA preparation and treatment. CsA was dissolved in the mixture of vehicle containing 90% olive oil and 10% ethanol. CsA solution was injected intraperitoneally with a final concentration of 30 mg/kg every 24 h, which started from 1 d before infection. Control mice were treated with the vehicle alone.

In vivo imaging analysis. Female BALB/c mice were used in experiments. Mice were intraperitoneally infected with 10^3 freshly egressed tachyzoites expressing luciferase resuspended in 100 µl PBS. For the local infection, mice were infected in the right hind footpad with 10^3 freshly egressed tachyzoites expressing luciferase resuspended in 50 µl PBS. Bioluminescence was assessed on the indicated days after infection. For the detection of bioluminescence emission, mice were intraperitoneally injected with 3 mg D-luciferin in 200 µl PBS (Promega), maintained for 5 min to allow for adequate dissemination of luciferin, and subsequently anaesthetized with isoflurane (Dainippon Sumitomo Pharma). At 10 min after injection of D-luciferin, photonic emissions were detected using an in vivo imaging system (IVIS-Spectrum; Xenogen) and Living image software (Xenogen).

Plaque assay. The WT and gra6-KO parasites were used to infect monolayers of MEFs seeded in 6-well plates. After incubation for 8–9 d at 37°C, cells were fixed with methanol for 10 min, followed by staining with crystal violet for 10 min.

Assessment of intracellular growth. MEFs seeded on cover glasses were inoculated with freshly released WT or gra6-KO parasites. At 24 h after infection, parasites were fixed with 4% PFA. Immunofluorescence assays were performed using α-TgGAP45 antibody, and parasites were counted on at least 100 vacuoles for each strain.

Generation of NFAT4-deficient mice by Cas9/CRISPR-mediated genome editing. The insert fragment of Nfat4 gRNA was amplified using KODFXNEO (Toyobo) and the primers (Fig. S1) Nfat4_gRNA1_F and Nfat4_gRNA1_R. The fragment for Nfat4 gRNA was inserted into the gRNA cloning vector (Plasmid 41824) using Gibson Assembly mix (New England Biolab) to generate Nfat4 gRNA-expressing plasmids. T7 promoter was added to the Nfat4 gRNA template using KODFXNEO and the primers Nfat4_T7gRNA_F and gRNA_common_R. The T7-Nfat4 gRNA PCR product was gel purified and used as the subsequent generation of Nfat4 gRNA. MEGAshortscript T7 (Life Technologies) was used for the generation of the Nfat4 gRNA. Cas9 mRNA was generated by in vitro transcription (IVT) using mMESSAGE mMACHINE T7 ULTRA kit (Life technologies) and the template that was amplified by PCR using pEF6-hCas9-Puro and the primers T7Cas9_IVT_F and Cas9_R (Ohshima et al., 2014), and gel-purified. The synthesized Nfat4 gRNA and Cas9 mRNA were purified using MEGAclear kit (Life Technologies) and eluted in RNase-free water (Nacalai Tesque).

To obtain *Nfat4*-mutated mice, B6C3F1 (C57BL/6 × C3H) female mice (6 wk old) were superovulated and mated to B6C3F1 stud males. Fertilized one-cell-stage embryos were collected from oviducts and injected into the pronuclei or the cytoplasm with 100 ng/µl Cas9 mRNA and 50 ng/µl Nfat4 gRNA in accordance with a previous study (Wang et al., 2013). The injected live embryos were transferred into oviducts of pseudopregnant ICR females at 0.5 d post coitus. The *Nfat4* loci of the resulting pups were screened using the primers Nfat4_indel_F and Nfat4_indel_R. The male pup harboring the mutation was mated to C57BL/6 female mice and tested for the germ line transmission. Heterozygotic mice for the mutated *Nfat4* locus were intercrossed to generate homozygotic *Nfat4*-deficient mice.

Tissue digestion and flow cytometry. Mice were infected into the footpads with *T. gondii*. Footpads and dpLNs of each group of mice at indicated times after infection were processed to obtain single-cell suspension. Footpads and dpLNs were digested at 37°C with shaking for 1 h (for footpads) or 25 min (for dpLNs) in the presence of 250 µg/ml Collagenase (Roche) and 50 µg/nl DNase (Roche). Then, samples were filtered through a 70-µm filter and used for FACS analysis. Single cell suspensions were pretreated with anti-CD16/32 (2.4G2) antibody to block Fc receptor and stained with anti-Ly6G (1A8; BD), anti-CD11b (M1/70, eBioscience), anti-CD45.2 (104; BD), and 7-AAD (BD). Stained cells were analyzed on a FACSVerse (BD) using FlowJo Software (Tree Star).

To obtain primary fibroblasts, tails of mice were excised and washed in PBS containing antibiotics. The tails were cut into small pieces, agitated, and digested with 4 mg/ml collagenase and 4 mg/ml DNase for 30 min at 37°C. Ice-cold complete DMEM was added to the resulting cell suspension. After centrifugation at 2,000 rpm for 5 min, pellets were resuspended in complete medium, and then cultured on dish. On the next day, the debris were collected and digested in 0.25% trypsin solution containing 400 nM EDTA for 30 min at 37°C. The resulting cell suspensions were added to the remaining

Published September 15, 2014

JEM

dish. Tail fibroblasts were used for detection of the chemokine mRNA expression in response to *T. gondii* infection by Q-PCR and NFAT4 protein by Western blotting.

Statistical analysis. The unpaired Student's *t* test and log-rank test were used to determine the statistical significance of the experimental data.

Online supplemental material. Fig. S1 shows primers used in this study. Online supplemental material is available at http://www.jem.org/cgi/content/full/jem.20131272/DC1.

We thank M. Enomoto and C. Hidaka for secretarial and technical assistance, and members of Yamamoto laboratory for discussion. We also thank Drs. Vern B. Carruthers and Dominique-Soldati Favre for providing us with Ku80-deficient type I *T. gondii* and anti-*T. gondii* antibodies, respectively.

This work was supported by grants from the Ministry of Education, Culture, Sports, Science and Technology, and Takeda Science Foundation; Senri Life Science Foundation; Tokyo Biochemical Research Foundation; Research Foundation for Microbial Diseases of Osaka University; Asahi Glass Foundation; Sumitomo Foundation; Sagawa Foundation of Promotion of Cancer Research; Suzuken Memorial Foundation; Osaka Cancer Research Foundation; Daiichi-Sankyo Foundation of Life Science; Uehara Memorial Foundation; Ichiro Kanehara Foundation; The Inoue Research Award; Mochida Memorial Foundation for Medical and Pharmaceutical Research; The Ichiro Kanehara Foundation; Kanae Fundation for the Promorion of Medical Science; Japan Intractable Disease Research Foundation; The Kao Foundation for Arts and Sciences (M. Yamamoto and M. Sasai); and Research Fellowships of Japan Society for the Promotion of Science for Young Scientists (J.S. Ma).

The authors declare no competing financial interests.

Submitted: 18 June 2013
Accepted: 7 August 2014

REFERENCES

Ahn, H.J., S. Kim, H.E. Kim, and H.W. Nam. 2006. Interactions between secreted GRA proteins and host cell proteins across the paratitophorous vacuolar membrane in the parasitism of *Toxoplasma gondii*. *Korean J. Parasitol.* 44:303–312. http://dx.doi.org/10.3347/kjp.2006.44.4.303

Appelberg, R. 1992. Macrophage inflammatory proteins MIP-1 and MIP-2 are involved in T cell–mediated neutrophil recruitment. *J. Leukoc. Biol.* 52: 303–306.

Awla, D., A.V. Zetterqvist, A. Abdulla, C. Camello, L.M. Berglund, P. Spégel, M.J. Pozo, P.J. Camello, S. Regnér, M.F. Gomez, and H. Thorlacius. 2012. NFATc3 regulates trypsinogen activation, neutrophil recruitment, and tissue damage in acute pancreatitis in mice. *Gastroenterology.* 143:1352–1360: e1–e7. http://dx.doi.org/10.1053/j.gastro.2012.07.098

Belfort-Neto, R., V. Nussenblatt, L. Rizzo, C. Muccioli, C. Silveira, R. Nussenblatt, A. Khan, L.D. Sibley, and R. Belfort Jr. 2007. High prevalence of unusual genotypes of *Toxoplasma gondii* infection in pork meat samples from Erechim, Southern Brazil. *An. Acad. Bras. Cienc.* 79:111–114. http://dx.doi.org/10.1590/S0001-37652007000100013

Bierer, R., C.H. Nitta, J. Friedman, S. Codianni, S. de Frutos, J.A. Dominguez-Bautista, T.A. Howard, T.C. Resta, and L.V. Bosc. 2011. NFATc3 is required for chronic hypoxia-induced pulmonary hypertension in adult and neonatal mice. *Am. J. Physiol. Lung Cell. Mol. Physiol.* 301:L872–L880. http://dx.doi.org/10.1152/ajplung.00405.2010

Bierly, A.L., W.J. Shufesky, W. Sukhumavasi, A.E. Morelli, and E.Y. Denkers. 2008. Dendritic cells expressing plasmacytoid marker PDCA-1 are Trojan horses during *Toxoplasma gondii* infection. *J. Immunol.* 181:8485–8491. http://dx.doi.org/10.4049/jimmunol.181.12.8485

Blanchard, N., F. Gonzalez, M. Schaeffer, N.T. Joncker, T. Cheng, A.J. Shastri, E.A. Robey, and N. Shastri. 2008. Immunodominant, protective response to the parasite *Toxoplasma gondii* requires antigen processing in the endoplasmic reticulum. *Nat. Immunol.* 9:937–944. http://dx.doi.org/10.1038/ni.1629

Boothroyd, J.C. 2009. *Toxoplasma gondii*: 25 years and 25 major advances for the field. *Int. J. Parasitol.* 39:935–946. http://dx.doi.org/10.1016/j.ijpara.2009.02.003

Boothroyd, J.C., and J.F. Dubremetz. 2008. Kiss and spit: the dual roles of *Toxoplasma* rhoptries. *Nat. Rev. Microbiol.* 6:79–88. http://dx.doi.org/10.1038/nrmicro1800

Bougdour, A., E. Durandau, M.P. Brenier-Pinchart, P. Ortet, M. Barakat, S. Kieffer, A. Curt-Varesano, R.L. Curt-Bertini, O. Bastien, Y. Coute, et al. 2013. Host cell subversion by *Toxoplasma* GRA16, an exported dense granule protein that targets the host cell nucleus and alters gene expression. *Cell Host Microbe.* 13:489–500. http://dx.doi.org/10.1016/j.chom.2013.03.002

Bram, R.J., and G.R. Crabtree. 1994. Calcium signalling in T cells stimulated by a cyclophilin B-binding protein. *Nature.* 371:355–358. http://dx.doi.org/10.1038/371355a0

Braun, L., M.P. Brenier-Pinchart, M. Yogavel, A. Curt-Varesano, R.L. Curt-Bertini, T. Hussain, S. Kieffer-Jaquinod, Y. Coute, H. Pelloux, I. Tardieux, et al. 2013. A *Toxoplasma* dense granule protein, GRA24, modulates the early immune response to infection by promoting a direct and sustained host p38 MAPK activation. *J. Exp. Med.* 210:2071–2086. http://dx.doi.org/10.1084/jem.20130103

Bushdid, P.B., H. Osinska, R.R. Waclaw, J.D. Molkentin, and K.E. Yutzey. 2003. NFATc3 and NFATc4 are required for cardiac development and mitochondrial function. *Circ. Res.* 92:1305–1313. http://dx.doi.org/10.1161/01.RES.0000077045.84609.9F

Cesbron-Delauw, M.F., C. Gendrin, L. Travier, P. Ruffiot, and C. Mercier. 2008. Apicomplexa in mammalian cells: trafficking to the parasitophorous vacuole. *Traffic.* 9:657–664. http://dx.doi.org/10.1111/j.1600-0854.2008.00728.x

Clipstone, N.A., and G.R. Crabtree. 1992. Identification of calcineurin as a key signalling enzyme in T-lymphocyte activation. *Nature.* 357:695–697. http://dx.doi.org/10.1038/357695a0

Cong, L., F.A. Ran, D. Cox, S. Lin, R. Barretto, N. Habib, P.D. Hsu, X. Wu, W. Jiang, L.A. Marraffini, and F. Zhang. 2013. Multiplex genome engineering using CRISPR/Cas systems. *Science.* 339:819–823. http://dx.doi.org/10.1126/science.1231143

Coombes, J.L., B.A. Charsar, S.J. Han, J. Halkias, S.W. Chan, A.A. Koshy, B. Striepen, and E.A. Robey. 2013. Motile invaded neutrophils in the small intestine of *Toxoplasma gondii*-infected mice reveal a potential mechanism for parasite spread. *Proc. Natl. Acad. Sci. USA.* 110:E1913–E1922. http://dx.doi.org/10.1073/pnas.1220272110

Courret, N., S. Darche, P. Sonigo, G. Milon, D. Buzoni-Gâtel, and I. Tardieux. 2006. CD11c- and CD11b-expressing mouse leukocytes transport single *Toxoplasma gondii* tachyzoites to the brain. *Blood.* 107:309–316. http://dx.doi.org/10.1182/blood-2005-02-0666

Dardé, M.L. 2004. Genetic analysis of the diversity in *Toxoplasma gondii*. *Ann. Ist. Super. Sanita.* 40:57–63.

Dardé, M.L. 2008. *Toxoplasma gondii*, "new" genotypes and virulence. *Parasite.* 15:366–371. http://dx.doi.org/10.1051/parasite/2008153366

Dubey, J.P., S.M. Gennari, N. Sundar, M.C. Vianna, L.M. Bandini, L.E. Yai, C.H. Kwok, and C. Suf. 2007. Diverse and atypical genotypes identified in *Toxoplasma gondii* from dogs in São Paulo, Brazil. *J. Parasitol.* 93:60–64. http://dx.doi.org/10.1645/GE-972R.1

Dubremetz, J.F. 2007. Rhoptries are major players in *Toxoplasma gondii* invasion and host cell interaction. *Cell. Microbiol.* 9:841–848. http://dx.doi.org/10.1111/j.1462-5822.2007.00909.x

Dunay, I.R., A. Fuchs, and L.D. Sibley. 2010. Inflammatory monocytes but not neutrophils are necessary to control infection with *Toxoplasma gondii* in mice. *Infect. Immun.* 78:1564–1570. http://dx.doi.org/10.1128/IAI.00472-09

Fazaeli, A., P.E. Carter, M.L. Darde, and T.H. Pennington. 2000. Molecular typing of *Toxoplasma gondii* strains by GRA6 gene sequence analysis. *Int. J. Parasitol.* 30:637–642. http://dx.doi.org/10.1016/S0020-7519(00)00036-9

Feliu, V., V. Vasseur, H.S. Grover, H.H. Chu, M.J. Brown, J. Wang, J.P. Boyle, E.A. Robey, N. Shastri, and N. Blanchard. 2013. Location of the CD8 T cell epitope within the antigenic precursor determines immunogenicity and protection against the *Toxoplasma gondii* parasite. *PLoS Pathog.* 9:e1003449. http://dx.doi.org/10.1371/journal.ppat.1003449

Gendrin, C., A. Bittame, C. Mercier, and M.F. Cesbron-Delauw. 2010. Post-translational membrane sorting of the *Toxoplasma gondii* GRA6 protein into the parasite-containing vacuole is driven by its N-terminal domain. *Int. J. Parasitol.* 40:1325–1334. http://dx.doi.org/10.1016/j.ijpara.2010.03.014

Hiller, N.L., S. Bhattacharjee, C. van Ooij, K. Liolios, T. Harrison, C. Lopez-Estraño, and K. Haldar. 2004. A host-targeting signal in virulence proteins reveals a secretome in malarial infection. *Science.* 306:1934–1937. http://dx.doi.org/10.1126/science.1102737

Howe, D.K., and L.D. Sibley. 1995. *Toxoplasma gondii* comprises three clonal lineages: correlation of parasite genotype with human disease. *J. Infect. Dis.* 172:1561–1566. http://dx.doi.org/10.1093/infdis/172.6.1561

Hu, M.S., J.D. Schwartzman, A.C. Lepage, I.A. Khan, and L.H. Kasper. 1999. Experimental ocular toxoplasmosis induced in naive and preinfected mice by intracameral inoculation. *Ocul. Immunol. Inflamm.* 7:17–26. http://dx.doi.org/10.1076/ocii.7.1.17.8109

Hunter, C.A., and L.D. Sibley. 2012. Modulation of innate immunity by *Toxoplasma gondii* virulence effectors. *Nat. Rev. Microbiol.* 10:766–778. http://dx.doi.org/10.1038/nrmicro2858

Jain, J., P.G. McCaffrey, Z. Miner, T.K. Kerppola, J.N. Lambert, G.L. Verdine, T. Curran, and A. Rao. 1993. The T-cell transcription factor NFATp is a substrate for calcineurin and interacts with Fos and Jun. *Nature.* 365:352–355. http://dx.doi.org/10.1038/365352a0

Kemp, L.E., M. Yamamoto, and D. Soldati-Favre. 2013. Subversion of host cellular functions by the apicomplexan parasites. *FEMS Microbiol. Rev.* 37:607–631. http://dx.doi.org/10.1111/1574-6976.12013

Khan, A., C. Jordan, C. Muccioli, A.L. Vallochi, L.V. Rizzo, R. Belfort Jr., R.W. Vitor, C. Silveira, and L.D. Sibley. 2006. Genetic divergence of *Toxoplasma gondii* strains associated with ocular toxoplasmosis, Brazil. *Emerg. Infect. Dis.* 12:942–949. http://dx.doi.org/10.3201/eid1206.060025

Kim, J.Y., H.J. Ahn, K.J. Ryu, and H.W. Nam. 2008. Interaction between parasitophorous vacuolar membrane-associated GRA3 and calcium modulating ligand of host cell endoplasmic reticulum in the parasitism of *Toxoplasma gondii*. *Korean J. Parasitol.* 46:209–216. http://dx.doi.org/10.3347/kjp.2008.46.4.209

Kong, J.T., M.E. Grigg, L. Uyetake, S. Parmley, and J.C. Boothroyd. 2003. Serotyping of *Toxoplasma gondii* infections in humans using synthetic peptides. *J. Infect. Dis.* 187:1484–1495. http://dx.doi.org/10.1086/374647

Labruyere, E., M. Lingnau, C. Mercier, and L.D. Sibley. 1999. Differential membrane targeting of the secretory proteins GRA4 and GRA6 within the parasitophorous vacuole formed by *Toxoplasma gondii*. *Mol. Biochem. Parasitol.* 102:311–324. http://dx.doi.org/10.1016/S0166-6851(99)00092-4

Lin, A., E.H. Shin, T.Y. Kim, J.H. Park, S.M. Guk, and J.Y. Chai. 2005. Genetic characteristics of the Korean isolate KI-1 of *Toxoplasma gondii*. *Korean J. Parasitol.* 43:27–32. http://dx.doi.org/10.3347/kjp.2005.43.1.27

Lopez-Rodríguez, C., J. Aramburu, A.S. Rakeman, and A. Rao. 1999. NFAT5, a constitutively nuclear NFAT protein that does not cooperate with Fos and Jun. *Proc. Natl. Acad. Sci. USA.* 96:7214–7219. http://dx.doi.org/10.1073/pnas.96.13.7214

Lu, B., B.J. Rutledge, L. Gu, J. Fiorillo, N.W. Lukacs, S.L. Kunkel, R. North, C. Gerard, and B.J. Rollins. 1998. Abnormalities in monocyte recruitment and cytokine expression in monocyte chemoattractant protein 1-deficient mice. *J. Exp. Med.* 187:601–608. http://dx.doi.org/10.1084/jem.187.4.601

Mack, D.G., and R. McLeod. 1984. New micromethod to study the effect of antimicrobial agents on *Toxoplasma gondii*: comparison of sulfadoxine and sulfadiazine individually and in combination with pyrimethamine and study of clindamycin, metronidazole, and cyclosporin A. *Antimicrob. Agents Chemother.* 26:26–30. http://dx.doi.org/10.1128/AAC.26.1.26

Marti, M., J. Baum, M. Rug, L. Tilley, and A.F. Cowman. 2005. Signal-mediated export of proteins from the malaria parasite to the host erythrocyte. *J. Cell Biol.* 171:587–592. http://dx.doi.org/10.1083/jcb.200508051

Martin, T., P.M. Cardarelli, G.C. Parry, K.A. Felts, and R.R. Cobb. 1997. Cytokine induction of monocyte chemoattractant protein-1 gene expression in human endothelial cells depends on the cooperative action of NF-χB and AP-1. *Eur. J. Immunol.* 27:1091–1097. http://dx.doi.org/10.1002/eji.1830270508

McCabe, R.E., B.J. Luft, and J.S. Remington. 1986. The effects of cyclosporine on *Toxoplasma gondii* in vivo and in vitro. *Transplantation.* 41:611–615. http://dx.doi.org/10.1097/00007890-198605000-00012

Melo, M.B., K.D. Jensen, and J.P. Saeij. 2011. *Toxoplasma gondii* effectors are master regulators of the inflammatory response. *Trends Parasitol.* 27:487–495. http://dx.doi.org/10.1016/j.pt.2011.08.001

Mercier, C., J.F. Dubremetz, B. Rauscher, L. Lecordier, L.D. Sibley, and M.F. Cesbron-Delauw. 2002. Biogenesis of nanotubular network in *Toxoplasma* parasitophorous vacuole induced by parasite proteins. *Mol. Biol. Cell.* 13:2397–2409. http://dx.doi.org/10.1091/mbc.E02-01-0021

Mercier, C., K.D. Adjogble, W. Däubener, and M.F. Delauw. 2005. Dense granules: are they key organelles to help understand the parasitophorous vacuole of all apicomplexa parasites? *Int. J. Parasitol.* 35:829–849. http://dx.doi.org/10.1016/j.ijpara.2005.03.011

Mikita, T., D. Campbell, P. Wu, K. Williamson, and U. Schindler. 1996. Requirements for interleukin-4-induced gene expression and functional characterization of Stat6. *Mol. Cell. Biol.* 16:5811–5820.

Miller, M.A., M.E. Grigg, C. Kreuder, E.R. James, A.C. Melli, P.R. Crosbie, D.A. Jessup, J.C. Boothroyd, D. Brownstein, and P.A. Conrad. 2004. An unusual genotype of *Toxoplasma gondii* is common in California sea otters (Enhydra lutris nereis) and is a cause of mortality. *Int. J. Parasitol.* 34:275–284. http://dx.doi.org/10.1016/j.ijpara.2003.12.008

Montoya, J.G., and J.S. Remington. 2008. Management of *Toxoplasma gondii* infection during pregnancy. *Clin. Infect. Dis.* 47:554–566. http://dx.doi.org/10.1086/590149

Müller, M.R., and A. Rao. 2010. NFAT, immunity and cancer: a transcription factor comes of age. *Nat. Rev. Immunol.* 10:645–656. http://dx.doi.org/10.1038/nri2818

Ohshima, J., Y. Lee, M. Sasai, T. Saitoh, J. Su Ma, N. Kamiyama, Y. Matsuura, S. Pann-Ghill, M. Hayashi, S. Ebisu, et al. 2014. Role of mouse and human autophagy proteins in IFN-γ-induced cell-autonomous responses against *Toxoplasma gondii*. *J. Immunol.* 192:3328–3335. http://dx.doi.org/10.4049/jimmunol.1302822

Oukka, M., I.C. Ho, F.C. de la Brousse, T. Hoey, M.J. Grusby, and L.H. Glimcher. 1998. The transcription factor NFAT4 is involved in the generation and survival of T cells. *Immunity.* 9:295–304. http://dx.doi.org/10.1016/S1074-7613(00)80612-3

Peixoto, L., F. Chen, O.S. Harb, P.H. Davis, D.P. Beiting, C.S. Brownback, D. Ouloguem, and D.S. Roos. 2010. Integrative genomic approaches highlight a family of parasite-specific kinases that regulate host responses. *Cell Host Microbe.* 8:208–218. http://dx.doi.org/10.1016/j.chom.2010.07.004

Petersen, E., B. Edvinsson, B. Lundgren, T. Benfield, and B. Evengård. 2006. Diagnosis of pulmonary infection with *Toxoplasma gondii* in immunocompromised HIV-positive patients by real-time PCR. *Eur. J. Clin. Microbiol. Infect. Dis.* 25:401–404. http://dx.doi.org/10.1007/s10096-006-0156-5

Peyron, F., J.R. Lobry, K. Musset, J. Ferrandiz, J.E. Gomez-Marin, E. Petersen, V. Meroni, B. Rausher, C. Mercier, S. Picot, and M.F. Cesbron-Delauw. 2006. Serotyping of *Toxoplasma gondii* in chronically infected pregnant women: predominance of type II in Europe and types I and III in Colombia (South America). *Microbes Infect.* 8:2333–2340. http://dx.doi.org/10.1016/j.micinf.2006.03.023

Pierre, K.B., C.M. Jones, J.M. Pierce, I.B. Nicoud, T.M. Earl, and R.S. Chari. 2009. NFAT4 deficiency results in incomplete liver regeneration following partial hepatectomy. *J. Surg. Res.* 154:226–233. http://dx.doi.org/10.1016/j.jss.2008.07.023

Reese, M.L., and J.C. Boothroyd. 2009. A helical membrane-binding domain targets the *Toxoplasma* ROP2 family to the parasitophorous vacuole. *Traffic.* 10:1458–1470. http://dx.doi.org/10.1111/j.1600-0854.2009.00958.x

Rosowski, E.E., D. Lu, L. Julien, L. Rodda, R.A. Gaiser, K.D. Jensen, and J.P. Saeij. 2011. Strain-specific activation of the NF-κB pathway by GRA15, a novel *Toxoplasma gondii* dense granule protein. *J. Exp. Med.* 208:195–212. http://dx.doi.org/10.1084/jem.20100717

Ruiz-Ortega, M., O. Lorenzo, and J. Egido. 2000. Angiotensin III increases MCP-1 and activates NF-κB and AP-1 in cultured mesangial and mononuclear cells. *Kidney Int.* 57:2285–2298. http://dx.doi.org/10.1046/j.1523-1755.2000.00089.x

Shastri, A.J., N.D. Marino, M. Franco, M.B. Lodoen, and J.C. Boothroyd. 2014. GRA25 is a novel virulence factor of *Toxoplasma gondii* and influences the host immune response. *Infect. Immun.* 82:2595–2605. http://dx.doi.org/10.1128/IAI.01339-13

Sibley, L.D., I.R. Niesman, S.F. Parmley, and M.F. Cesbron-Delauw. 1995. Regulated secretion of multi-lamellar vesicles leads to formation of a tubulo-vesicular network in host-cell vacuoles occupied by *Toxoplasma gondii*. *J. Cell Sci.* 108:1669–1677.

Silverman, J.M., S.K. Chan, D.P. Robinson, D.M. Dwyer, D. Nandan, L.J. Foster, and N.E. Reiner. 2008. Proteomic analysis of the secretome